Review of “US East Coast synthetic aperture radar wind tlas for offshore wind energy” by Ahsbahs et al, submitted to Wind Energy Science Discussions

The paper provides the first atlas of the offshore wind resource along the US East Coast derived from high spatial resolution (2 km) SAR products from four satellites at 10 m above sea level. A detailed comparison against two independent data source is also provided, buoys and WIND Toolkit, as well as a discussion of biases, seasonality, and gradients. This is one of the best papers I have ever reviewed and it should definitely be published soon. I only have a few minor comments and suggestions.

Answer: Thank you very much for a fast and very positive review. We highly appreciate your constructive comments and have followed them all as specified in the following.

1. It was not until page 5 (line 15) that the 10-m height was mentioned. It is important to let the reader know that the atlas is valid at 10 m asl earlier than that. I recommend that you add this information in the abstract (“We present the first synthetic aperture radar (SAR)-based, offshore, 10-m wind atlas …”) and even in the Introduction around p. 2 lines 20-30.

Answer: Agreed. We have added this information to the abstract and the introduction.

2. Similarly, you need to mention the height of the buoy measurements in section 2.3 (it is mentioned later (p. 6 line24) but it should be here) and the height of the WIND Toolkit output in section 2.4 (10 m – is this a real model level or an interpolated value? If interpolated as I think, how?)

Answer: Buoy measurements are at heights between 2 and 7 m above the sea level. We have added sentences at your suggested locations. The 10m wind variables from WRF are used directly.

3. In the abstract, the WRF model is mentioned, but also the WIND Toolkit project should be mentioned, otherwise the reader thinks that the authors ran the WRF model themselves. Instead, they used WIND, which is a well-documented, publicly available dataset.

Answer: We have added this in the abstract and modified the sentence to: “The SAR wind atlas is used as a reference to study wind resources derived from the Wind Integration National Dataset Toolkit (WTK), which is based on seven years of modelling output from the Weather Research and Forecasting (WRF) model.” Throughout the rest of the manuscript, we have used ‘WTK’ consistently about this data set.

4. P. 2 , l. 19: a noun is missing “SAR-derived [what?] show…”

Answer: It is SAR derived wind speeds. We have corrected the sentence to:

“It has been shown that SAR-derived winds can accurately depict wind speed gradients measured by ground based lidars near the coastline (Ahsbahs et al., 2017) and that SAR wind fields show similar mean wind speed variations as those experienced by wind turbines (Ahsbahs et al., 2018).”

5. P. 4, l. 5: what is a “scene”? A snapshot? A picture?

Answer: In principle, the same scene can be observed from different angles; each leading to their own image. As we are only looking at co-polarized images here, these terms are almost interchangeable. We have changed all occurrences of "scene" to "SAR image" as this is more understandable for the wind energy community.

6. P. 5, l. 13: what exactly is the "normalized radar cross section of the ocean surface"? I am unclear on what exactly it is that the SAR measures on the ocean surface. Is it a reflectivity of some sort? Is it related to white caps of the waves? Please add a brief description here. Also, briefly describe how the GMF works.

Answer: The normalized radar cross section is the quantity for the radar backscatter per unit area. GMFs are empirical functions relating the radar backscatter to the wind speed. We have tried to clarify this to the reader:

"SAR wind retrievals from the database of the Technical University of Denmark are used for this study and their processing is described in the following. SAR images are measures of the radar backscatter from the Earth's surface. The intensity of this backscatter is commonly referred to as the normalized radar cross section (NRCS). Level-1 SAR data are downloaded from the data providers and calibration is applied to obtain the NRCS. The processing is done using the SAR Ocean Products System (SAROPS) software package (Monaldo et al., 2014). Radar backscatter and thus the NRCS of the ocean surface is determined by Bragg scattering (Valenzuela, 1978). This scattering mechanism is most sensitive to wave lengths on the order of 10 cm. At this scale, waves can be assumed to be in local equilibrium with the wind speed and therefore, the NRCS and the wind speed are correlated. An empirical Geophysical Model Function (GMF) can link the NRCS and additional radar parameters to the wind speed at 10 m height above the sea surface."

7. P. 5, l. 20. Either a period "." is missing (before "Climate Forecast…") or the phrase is incomplete. It's good that it was not the WIND's wind direction that was used here.

Answer: We have rephrased to:

"Two sources of wind directions are used for the SAR wind retrieval: until 2010, wind directions come from the National Center for Atmospheric Research Climate Forecast System Reanalysis (CFSR) reanalysis data and from 2011 onwards, wind directions from the Global Forecast System (GFS) are used."

8. P. 6, l. 25: briefly describe how the extrapolation from 5 m to 10 m is calculated in the COARE 3.0 algorithm for the buoy data.

Answer: We have added the following sentences and a reference to briefly describe this algorithm:

"In this algorithm, atmospheric stratification is described using the difference between the air and sea temperature together with empirically found constants. The wind speed is then extrapolated considering atmospheric stability and roughness as described by Charnock's relation (Charnock, 1955)."

9. Figs. 2 and 3: what are the black lines with vertical error bars? Medians? Please add info in the captions.

Answer: The black lines indicate the mean SAR wind speed per wind speed bin (binned by buoy winds) and one standard deviation. We have added a description to the text:

"SAR wind speeds are split into 1 m/s bins according to the buoy wind speed. The SAR mean wind speed and standard deviation around this mean are calculated and plotted as well."

And in the caption of the two figures:

“The black curves indicate the mean within each 1 m/s bin and the vertical lines around the mean value indicate one standard deviation within this bin.”.

10. Fig. 4: please use the same color bar for Fig. 4a and 4b. They are similar but not identical in the current figure.

We changed this. A GIS team NREL is remaking the plots with nicer plotting libraries.

11. Fig. 7: the month of “Feb” should be capital.

Answer: We have made the change.

12. P. 27, l. 4: missing noun after “from”, maybe “SAR”?

Answer: We have rephrased to “Mean wind speed maps from SAR and WTK have been compared in this study.”

13. Future work, item ii). I do not agree with this recommendation, remove it or explain it better. Why would randomly sampling model output, which actually includes seasonal and diurnal variability correctly, be a better way to present a wind atlas? This procedure would mimic the SAR behavior, but it would not necessarily provide a better estimate of the actual wind resource. I think the authors are saying that this random sampling method would be a better to validate SAR, not a better way to represent the wind resource. If so, please clarify/rephrase

Answer: We agree so we have revised the section on future work completely and removed this point. The focus is now on future perspectives for SAR-based wind atlases alone:

“With an increasing archive of Sentinel-1 data, future wind atlases will be based on samples, which are more distributed over the time of day. The rapid growth of our SAR data archives over time will in itself improve the accuracy of wind resource statistics. Further, a weighting of the SAR scenes by month could partly overcome seasonal biases and give better estimations of the Weibull parameters while retaining the observational character of a SAR-based wind atlas.”

Interactive comment on “US East Coast synthetic aperture radar wind atlas for offshore wind energy” by Tobias Ahsbahs et al.

SUMMARY

This is a valuable manuscript demonstrating data quality control and analysis meth- ods that should be of considerable use to the offshore wind energy community. The manuscript provides a well described application of methods from prior studies to the offshore waters of the United States’ East Coast. The downside of this approach is that the current study retains all of the meteorological and statistical shortcomings of these existing methods. The advanced data sources, particularly WRF model analyses, used in this study, provide the authors with a, so far, unexploited opportunity to correct these short comings and set a new standard for SAR wind power analysis. My comments below focus on highlighting these opportunities.

Answer: Thanks very much for giving this manuscript a thorough review and for the constructive suggestions for its improvement.

STRENGTHS

- Good choice of geophysical model function OPPORTUNITIES

Answer: Thanks!

Opportunity 1 - Neutral vs stratified surface layer.

A longstanding challenge in SAR wind analysis has been that neutral stratification of the surface layer "must" be assumed. This has resulted in SAR retrieval algorithms returning estimates of neutral-equivalent wind rather than of true wind. The resulting neutral-equivalent wind is actually a proxy for surface stress, just expressed as wind via the neutral drag law.

The effect of this assumed neutral stratification of the surface layer is a wind speed bias that depends on the stability of the atmospheric surface layer. The SAR-derived wind speeds are too low in regions where the surface layer is stable, because wind speed must compensate for the too high (i.e. neutral rather than stable) drag coeffi- cient assumed. Likewise, the SAR-derived wind speeds are too high in regions where the surface layer is unstable, because wind speed must compensate for the too low (i.e. neutral rather than unstable) drag coefficient assumed. Basically, SAR-derived wind is having to compensate for the lack of the stability dependence of the vertical mixing of momentum in the surface layer. This is reflected in the present study in the observation that SAR winds are faster than buoy winds over the Gulf Stream (where the atmospheric surface layer is destabilized by the warm underlying water) and slower than the buoy winds over the cold waters north of the Gulf Stream (where the atmo- spheric surface layer is stabilized by the cool underlying water).

For most of the history of SAR, that was the best anyone could do, because there were no good sources for surface layer stability estimates over the ocean. This study, however, has the access to WRF analyses from which surface layer stability can be easily calculated. In Section 3.2.1 - The TOGA COARE bulk flux algorithm is used to account for the effects stability on the vertical extrapolation of buoy winds. This same stability correction could be used to convert SAR-derived surface stress to stability- aware SAR-derived winds. All it would take would be to use the neutral drag law to convert the neutral-equivalent SAR-derived winds to surface stress and then the equa- tions from the TOGA COARE bulk flux algorithm to convert that surface stress back to a stability-aware 10 m wind. This would be a major advance for SAR wind analysis, one the authors are perfectly positioned to make given that they are already using both WRF analyses (from which surface layer stability can be calculated) and the TOGA COARE bulk flux algorithm which allows their affects on the flux/wind relationship to be computed. Locations where this issue comes up include: Page 2 lines 14-15 Page 5, line 15 Section 3.2.1 - all Page 11, lines 15-16 Page 13, Line 12 Page 17, Figure 8 - The Gulf Stream's northwest edge is so prominent in this figure precisely because of the lack of stability correction in the neutral-equivalent SAR-derived winds. Page 18, Figure 9 - Same. Page 20, lines 12-14 - This is another sign that the change in surface layer stability across the northwest edge of the Gulf Stream is contributing to the gradient in neutral-equivalent SAR-derived winds observed there. Page 21, line 4 - This is due to the cross-talk between surface layer stability and neutral-equivalent SAR-derived winds. Page 25, lines 22-24 - Here is where you basically outline the method I'm suggesting above. In short, you're most of the way there already, so you might as well make the advance and claim the glory.

Answer: We are grateful to receive this concrete and detailed suggestion for an opportunity, we could take. Although it seems simple to apply air-sea temperature differences in combination with the TOGA COARE algorithm in order to correct the SAR winds for atmospheric stability, we have chosen not to pursue this opportunity in the present manuscript for the following reasons:

- We would like to keep the SAR and WTK data sets completely independent since the main objective of our analyses is to compare the two data sources and explore their strengths and weaknesses in connection with wind resource assessment.

- Previous research indicates that WRF outputs are not so suitable for stability correction of instantaneous wind speed profiles whereas they can be used with confidence for correction of the long-term average wind speed (Pena & Hahmann, 2012, https://onlinelibrary.wiley.com/doi/full/10.1002/we.500; Badger at al., 2016, https://doi.org/10.1175/JAMC-D-15-0197.1).

- The best way to persue the suggested opportunity would, in our oppinion, be to first validate the air and sea temperatures from WTK (WRF) against the ocean buoy observations. If their accuracy is satisfactory, the TOGA COARE algorithm could be applied, as suggested here, and both the uncorrected and corrected wind speeds could then be compared against the buoy observations of wind speed. Altogether, this would be a substantial amount of analyses, which would deserve a separate publication. Given that both the ocean buoy observations and the WTK are open data sets and that the US East Coast remains highly relevant for offshore wind energy developments, we would be very interested in continuing our efforts in the near future.

We have taken the liberty to use paragraphs of text from the reviewer's comments directly in the manuscript in order to properly describe and discuss the issue of atmospheric stability effects. In the discussion:

“A longstanding challenge in SAR wind analysis has been that neutral stratification of the surface layer must be assumed. The effect of this assumed neutral stratification of the surface layer is a wind speed bias that depends on the stability of the atmospheric surface layer. The SAR-derived wind speeds are too low in regions where the surface layer is stable, because wind speed must compensate for the too high (i.e. neutral rather than stable) drag coefficient assumed. Likewise, the SAR-derived wind speeds are too high in regions where the surface layer is unstable, because wind speed must compensate for the too low (i.e. neutral rather than unstable) drag coefficient assumed. Basically, the SAR-derived wind is having to compensate for the lack of the stability dependence of the vertical mixing of momentum in the surface layer. This is reflected in our study in the observation that SAR winds are faster than buoy winds over the Gulf Stream (where the atmospheric surface layer is destabilized by the warm underlying water) and slower than the buoy winds over the cold waters north of the Gulf Stream (where the atmospheric surface layer is stabilized by the cool underlying water). Results from earlier resource assessments in Dvorak et al. (2013) using WRF show that wind resources are generally increasing going from south to north in our investigated domain but show less variability than both SAR and WTK”.

And in the section on future work:

“This study has utilized the COARE 3.0 bulk flux algorithm to account for the effects of atmospheric stability on the vertical extrapolation of buoy winds. This same stability correction could be used to convert the SAR-derived surface stress to stability-aware SAR winds given that the air-sea temperature difference for any point in the area of interest can be obtained from the WTK data set. The neutral drag law could be used to convert the neutral-equivalent SAR-derived winds to surface stress and then the equations from the COARE 3.0 bulk flux algorithm could be applied to convert that surface stress back to a stability-aware 10 m wind. This would be a major advance for SAR wind analysis and represents a natural next step for our analysis of wind resources along the US East Coast.”

Opportunity 2 - Weighting cases in Weibull fitting

The authors wisely weight cases to equalize monthly contributions to the mean, but forebear from doing so when fitting the Weibull distribution parameters. I was curi-ous if this latter process was as hard as the authors assumed, so I looked up how Weibull distributions are fit and discovered that weighting data from different months differently in finding the parameters of a Weibull distribution should be straightforward.

See the link below for a clear discussion of how the method of moments is used to find the Weibull parameters. http://www.real-statistics.com/distribution-fitting/method- of-moments/method-of-moments-weibull/ Since the inputs to this method are just mean and standard deviation, both of which can be computed with weighted observations, Weibull distributions can be fit with weighted observations with very little coding effort.

Publishing this trivial, but currently unused advance would be of great help to the SAR wind climatology community and would also impact other meteorological communities which are using the method of moments to fit various distributions to data that is un- evenly distributed in space or time.

Answer: We agree that it is, in principle, not hard to use the method of moments to recalculate the Weibull parameters and the energy densities based on the weighted wind speed values. The issue is more of a practical nature as we have used the DTU-software S-WAsP for the Weibull fitting, which is no longer maintained or updated. The tool does not include functionalities for weighting of SAR wind data. The main advantage of using the S-WAsP tool is its ability to handle large amounts of satellite data and projecting the wind maps on a regular grid before the calculation of Weibull parameters etc. Work is in progress to build a new system based on NetCDF files and Python coding. Until this is ready, it would require a significant effort to recalculate the Weibull parameters for the 6,500+ SAR scenes in this analysis. We have removed this sentence about S-WAsP from the manuscript as it probably leads to confusion rather than clarification:

"S-WAsP is not able to account for seasonal biases in the Weibull parameter estimation. Therefore, no seasonally corrected Weibull parameters or energy densities are available".

Further, we have revised the section on future work to address the issue of sampling biases more clearly using the reviewer's formulation directly:

"With an increasing archive of Sentinel-1 data, future wind atlases will be based on samples, which are more distributed over the time of day. The rapid growth of our SAR data archives over time will in itself improve the accuracy of wind resource statistics. Further, a weighting of the SAR scenes by month could partly overcome seasonal biases and give better estimations of the Weibull parameters while retaining the observational character of a SAR-based wind atlas. Such an advance would be of great help to the SAR wind climatology community and would also impact other meteorological communities which are using the method of moments to fit various distributions to data that is unevenly distributed in space or time."

MINOR ITEMS

Page 1, line 22 - "vary" is vague. Some readers will read this sentence as meaning the mean wind speed is under 1 m/s rather than the intended meaning of the mean wind speed varying by this much across a wind-farm lease area. This issue of too general terms being used for statistics for which precise terms or phrases are available recurs in this manuscript. I have attempted to point out each location where reader confusion may arise.

Answer: We have tried to make this specific sentence more clear to the reader and changed it to:

"Areas designated for offshore wind development by the Bureau of Ocean Energy Management are investigated in more detail; the wind resource in terms of the mean wind speed show spatial variations within each designated area between 0.3 and 0.5 m/s for SAR and less than 0.2 m/s for the WTK."

Thank you for spotting this general weakness; we have tried to focus on precision while revising the manuscript.

Page 2, line 16 - "at scales around" - This wording will make most readers think the resolution rather than the swath width is several hundred kilometers.

Answer: Agreed. We have clarified this while avoiding too satellite specific terms, as the audience is considered to have more of a wind energy background. Changed to. “Scatterometers and synthetic aperture radar (SAR) on board satellites provide coverage over several hundred kilometers and it is possible to retrieve wind speeds at 10 m above sea level from radar backscatter of the ocean surface.”

Page 3, line 1 - "variation" is too vague a term. Please specify if you mean temporal or spatial variation and over what time or space scale.

Answer: We have clarified that this is the spatial variation and that scales are approximately a kilometer. The sentence has been changed to:

“Lastly, the spatial variation of mean wind speeds on the kilometre scale are investigated for BOEM lease areas designated for wind farm development.”

Page 4, Table 1 - I suspect most readers would like a column with SAR pixel size. Also, incidence angle and swath width need units. Degrees and Kilometers, I suspect.

Answer: We have added the units, thank you for spotting this. This paper is aimed for the audience of wind energy researchers and industry. We do not think that the pixel size is relevant for them as the data presented is averaged to 500m pixels before performing the wind retrieval.

Page 5, Section 2.4 - It is not clear from this paragraph how these pieces fit together. In particular, it should be made clear whether or not WRF part of WTK?

Answer: We have revised section 4.2 and also parts of the abstract and introduction with respect to WTK in order to make it clear that WRF is the model used to create the WTK data set. We now use the abbreviation ‘WTK’ consistently each time we talk about this data set (previously, we also used the naming ‘WIND Toolkit’ and occasionally ‘WRF’).

Page 5, lines 19-21 - Please explain why the data source switched.

Answer: We have added an explanation:

“The switch in wind direction input is present in the database of derived SAR wind maps due to a change to near real time processing.”

We now introduce the paragraph by stating the use of a pre-existing data base:

“SAR wind retrievals from the database of the Technical University of Denmark are used for this study and their processing is described in the following.”

Page 6, lines 7-8 - "from modeled wind speeds" - It would help readers to know which modeling system you’re referring to here.

Answer: It is the same modelled winds as used for the wind retrieval algorithm. We have added this sentence:

“NRCS are calculated from the modelled winds that are used for the SAR wind inversion described in Section 2.4 and compared to the SAR measurements”

Page 8, lines 6-8 - What are these numbers and why are they being discussed here. Are they extreme cases? Means? The discussion is to too terse for clarity.

Answer: We have expanded the description order to point out that the overall bias may be close to zero but there are positive and negative biased for specific wind speed intervals for Envisat in particular:

"The two largest data sets, Envisat (b) and Sentinel-1A AC (e), show a higher mean wind speed from SAR when the buoy wind speed is less than 7 m/s and vice versa lower mean wind speeds from SAR when buoy wind speeds exceed 9 m/s. For Envisat, these opposing biases are averaged to nearly zero in the overall bias".

Page 10, paragraph below the second equation - Would it be better to aggregate spatially before fitting the Weibull distribution rather than after? One worries about the order of fitting and smoothing when the fitting is a nonlinear process as it is in this second order moment approach. This is an issue of Jensen's Inequality, I think.

Answer: This is in fact done in our analysis. We have moved the relevant description so it is now above the equation to clarify that the spatial mean is taken before the Weibull fit:

"SAR wind images are projected on a regular WGS84 grid with 0.02° cell spacing before processing the data to a wind atlas."

Page 13, line 12 - While the difference is small in the mean, that is in all likelihood because stable cases and unstable cases are roughly equally likely. The stability impact on the tails of the distribution could thus be quite large. The spatial distribution of biases noted by the authors speak strongly to the impact of surface layer stability on the errors in neutral-equivalent SAR-derived winds, even in the mean.

Answer: We agree with this point and have tried to include it in the discussion and future work sections - see our answer to 'Opportunity 1' above.

US East Coast synthetic aperture radar wind atlas for offshore wind energy

Tobias Ahsbahs[1], Galen Maclaurin[2], Caroline Draxl[2], Christopher R. Jackson[3], Frank ~~Monaldo[3]~~Monaldo[4], Merete Badger[1]

[1] DTU Wind Energy, Risø, Roskilde, Denmark

[2] National Renewable Energy Laboratory, Golden, Colorado, USA

[3] Global Ocean Associates, Alexandria, VA USA

[4] Applied Physics Laboratory, Johns Hopkins University, Baltimore, Maryland, USA

Correspondence to: ~~Tobias Ahsbahs ttah~~Merete Badger mebc@dtu.dk

Abstract

We present the first synthetic aperture radar (SAR~~) based~~) offshore wind atlas of the US East Coast from Georgia to the Canadian border. Images from Radarsat-1, Envisat, ~~Sentinel-1A,~~ and Sentinel-~~1B~~1A/B are processed to wind maps using the Geophysical Model Function (GMF) CMOD5.N. Extensive comparisons with 6,008 collocated buoy observations ~~revealed~~of the wind speed reveal that biases of the individual ~~system~~systems range from -0.8 to 0.6 m/s. Unbiased wind retrievals are crucial for producing an accurate wind atlas and intercalibration ~~for correcting these biases by adjusting~~of the ~~normalized radar cross section~~SAR observations is therefore applied. ~~The~~Wind retrievals from the intercalibrated SAR observations show biases in the range of to -0.2 to 0.0 m/s, while at the same time improving the root mean squared error from 1.67 to 1.46 m/s. ~~These~~The intercalibrated SAR observations are, for the first time, aggregated to create a wind atlas~~. Monthly averages are used to correct artefacts from seasonal biases.~~ at the height 10 m above sea level. The SAR wind atlas is used as a reference to study wind resources derived from the Wind Integration National Dataset Toolkit (WTK), which is based on seven years of modelling output from the Weather Research and Forecasting (WRF) model. Comparisons focus on the spatial variation of wind resources and show that model ~~results estimate~~outputs lead to lower coastal wind speed gradients than those derived from SAR. ~~At sites~~Areas designated for offshore wind development by the Bureau of Ocean Energy Management~~,~~ are investigated in more detail; the wind resource in terms of the mean wind ~~speeds typically vary~~speed show spatial variations within each designated area between 0.3 and 0.5 m/s for SAR and less than 0.2 m/s for the ~~WRF model within each site. Findings~~WTK. Our findings indicate that wind speed gradients and ~~variation~~variations might be underestimated in mesoscale model outputs along US East Coast.

1 Introduction

Offshore wind energy has been established on the continental shelf of Northern Europe since 2001 with a total installed capacity of 15,780 MW (Wind Europe, 2018). The US East Coast is similar in water depths and population density and could thus be well-suited for offshore wind farms (Kempton et al., 2007). During the past decade, the Bureau of Offshore Energy Management (BOEM) has leased out areas designated for offshore wind farm development along the US East Coast (BOEM, 2018), and the first wind plant became operational in 2016 (Block Island Wind Farm, Rhode Island[1]). Accurate and long-term wind statistics across broad geographic ~~extents~~areas (i.e., wind atlases) are needed to support offshore wind energy deployment. Wind atlases can be developed from local in situ measurements, i.e., buoys or meteorological masts (Troen and Petersen, 1989); numerical weather prediction models; (Dvorak et al., 2013; Hahmann et al., 2015); or satellite-based remote sensing (Christiansen et al., 2006; Hasager et al., 2015). ~~The objective of this study is to create and validate a satellite-based offshore wind atlas for the US East Coast and compare it to results from numerical weather prediction models.~~

Offshore wind resource data for the US East Coast are available from the Weather Research and Forecasting (WRF) model (Draxl et al., 2015b; Dvorak et al., 2013). For offshore wind energy, locations close to shore are most attractive because installation costs increase with the distance to shore because of increased water depth and longer cables. The BOEM lease areas are mainly located in coastal waters less than 70 km from shore where influences from upstream land masses are still substantial (Barthelmie et al., 2007) and mesoscale models can result in high uncertainties (Hahmann et al., 2015). These models need validation. Colle et al. (2016) point out that observations at turbine hub heights around 100 m are lacking and provide case-study-based validation using observations from airplanes. Long-term reference wind climates at broad geospatial scales are missing because observations from ocean buoys are sparse. ~~Radar images from~~

Scatterometers and synthetic aperture radar (SAR) on board satellites provide ~~measurements~~coverage over ~~large areas~~several hundred kilometers and it is possible to ~~infer~~retrieve wind speeds at 10 m from ~~the~~ radar backscatter of the ocean surface. ~~Scatterometers and synthetic aperture radar (SAR) can measure wind speeds following this principle at scales around several hundred kilometers.~~ SAR is better suited for resolving ~~wind resources~~winds in coastal zones because of its higher spatial resolution (Christiansen et al., 2006). It has been shown that SAR-derived winds can accurately depict wind speed gradients ~~outwards from 1 km offshore~~measured by ground based lidars near the coastline (Ahsbahs et al., 2017) and that SAR ~~-derived~~ wind fields show similar mean wind speed variations as those experienced by ~~a~~ wind turbines (Ahsbahs et al., 2018).

Wind resources can be assessed from SAR (Christiansen et al., 2006) and studies have been performed at different locations (Doubrawa et al., 2015; Hasager et al., 2011). For the US East Coast, a SAR-based wind atlas has been created from Radarsat-1 (RS1) data for a small area off the coast of Delaware (Monaldo et al., 2014). Expanding this study to the entire US East Coast with RS1 data is not possible because the images were acquired specifically for this ~~region~~atlas and coverage outside this region is limited. ~~We~~Here, we have ~~acquired~~collected additional data from Envisat (ENV), Sentinel-1A (S1A), and

[1] http://dwwind.com/project/block-island-wind-farm/

Sentinel-1B (S1B) ~~that~~which are distributed via Copernicus services. These data are openly available to public research, which is not the case for data from other SAR missions such as TerraSAR-X, Cosmo SkyMed, or Radarsat-2.

The objective of this study is to create and validate a satellite-based offshore wind atlas for the US East Coast and compare it to outputs from numerical weather prediction models.

The objective of this article is to produce and validate a SAR~~ observation~~-based wind atlas for the US East Coast by merging observations from four different satellites. We will remove possible offsets between wind retrievals from the different SAR sensors and validate ~~this by comparing~~the intercalibrated data set through comparisons with ~~data~~observations from the well-established ocean buoy network on the US East Coast. ~~For comparison, we~~The SAR-based wind atlas will ~~use~~be compared to data from the Wind Integration National Dataset ~~(WIND) toolkit~~Toolkit (WTK) produced by the National Renewable Energy Laboratory (NREL) from 7 model years of outputs from the Weather Research and Forecasting (WRF~~ outputs~~) model (Draxl et al., 2015b). The WTK is a state of the art mesoscale model run specifically focused on parameters important for wind energy production. We focus on coastal wind speed gradients and determine how they are represented in wind atlases from SAR and WTK. Lastly, the spatial variation of mean wind ~~speed variation is examined within~~speeds on the kilometre scale are investigated for BOEM lease areas designated for wind farm development.

The article is structured as follows: Section 2 provides an overview of the data and the area of interest ~~of~~for this study. Section 3 describes the methods used to create a SAR-based wind atlas. Section 4 presents wind climatologies and measurement artefacts of the SAR wind atlas. Section 5 focuses on using the SAR wind atlas to investigate wind variations and compares to the WTK. Sections 6 ~~and 7 further discusses~~contains a discussion of the results and ~~draws~~in Section 7, we draw conclusions on the potential use of the wind atlas.

2 Data and area of interest

2.1 Area of interest

We focus this study on coastal waters off the US East Coast from Georgia to the Canadian border. The area of interest is defined as between 30.7° and 45° latitude and -63° and -81.3° longitude extending ~~out~~ 400 km offshore, as shown in Figure 1. The positions of ocean buoys ~~described in Section 2.3~~within the area are shown as well~~.~~ (see also Section 2.3).

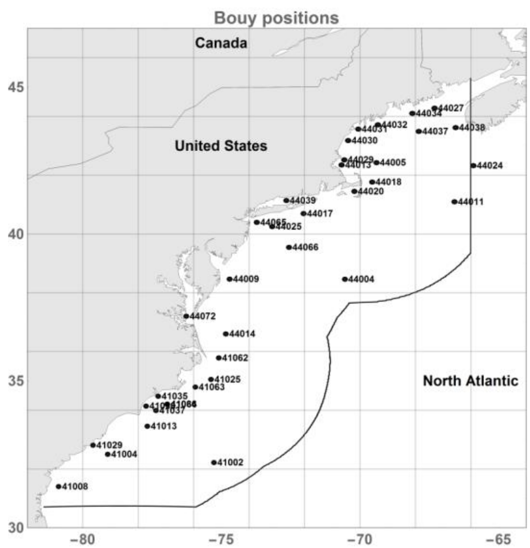

Figure 1: Area of interest for this study and <u>ocean</u> buoy positions.

2.2 Synthetic aperture radar

Satellites carrying SAR instruments have been operational for decades and extensive <u>image</u> archives exist. Portions of these archives can be used by the scientific community and <u>the</u> European Space Agency (ESA) archives are becoming increasingly open via Copernicus[2] services. SAR sensors usually operate in different modes depending on the desired <u>spatial</u> resolution of the images. We focus on modes that offer the widest possible swaths, because ~~the~~<u>our</u> aim is to create broad-scale wind resource maps. Co-polarized images in VV and HH mode from Envisat's wide swath mode (WSM), Sentinel-1's extra wide (EW) and interferometric wide (IW) modes, and Radarsat-1's ScanSAR wide (WD1) mode are used throughout this study (Table 1). The number of ~~scenes~~<u>images</u> can be misleading when assessing the coverage of each sensor, because the length of the swath varies (Envisat ~~scenes~~<u>images</u> tend to be more than ten times longer than Sentinel-1 ~~scenes~~<u>images</u>). Sentinel-1A~~ and ~~<u>/</u>B are operational at the moment and data ~~to~~<u>until</u> May 2018 are included.

Table 1: Overview of SAR sensors and the respective imaging modes and properties. The period of operation and number of ~~scenes~~<u>images</u> included in this study are also shown.

Satellite	Mode	Polarization	Incidence<u>[°]</u>	Swath width <u>[km]</u>	Period	~~Scenes~~<u>Number of images</u>

Formatted Table

[2] https://www.copernicus.eu/de

Envisat	WSM	VV	18–45	405	2002–2012	2198
		HH	18–45	405		513
Sentinel-1A	IW	VV	30–45	250	2015–2018	2403
	EW	HH	30–45	400		27
Sentinel-1B	IW	VV	30–45	250	2015– 2018	517
Radarsat-1	WD1	HH	20–45	400	1996–2008	924

2.3 Buoy data

High-quality wind and temperature measurements are available on the US East Coast from the buoy center of the National Oceanic and Atmospheric Administration (NOAA) (National Data Buoy Center, 1971). ~~These will be~~

Wind measurements at the buoy stations are obtained at various heights between 2 and 7 m above sea level. The buoy observations are used here as reference measurements. We only use buoys located more than 5 km from the ~~shore~~shoreline to avoid possible land contaminations in the corresponding SAR images~~. Measurements from~~. A total of 31 buoys ~~are used in~~fulfil this ~~study~~criterion and ~~the~~their approximate locations are shown in Figure 1. ~~Buoys~~The majority of the buoys are~~ mainly~~ located within 100 km from the ~~shore. Wind~~ shoreline. Locations and measurement heights are recorded annually in the buoy data files but changes can occur within a year. Additional metadata on buoy positions and measurement heights are available and represent the most accurate information according to NOAA (National Data Buoy Center, 2015). We use the information given in the metadata. Buoy wind speeds and ~~direction~~directions are measured every hour for 8 minutes and data are automatically quality controlled (National Data Buoy Center, 2009). ~~We performed additional quality control by checking time periods where SAR wind retrievals showed more than 10 m/s difference. Four periods are removed from specific buoys that showed unrealistically low wind speeds in the buoy measurements for several months and one short period where the buoy measurements are unreasonably high. Locations and measurement heights are recorded annually in the buoy file but changes can occur within a year. Additional metadata on buoy position and measurement heights are available that represent the most accurate information according to the NOAA buoy center (National Data Buoy Center, 2015). The more accurate metadata have been used.~~We perform additional quality control through manual inspection of data points where the difference between SAR and buoy wind speeds exceed 10 m/s. This leads to removal of four periods from specific buoys that show unrealistically low wind speeds for several months and one short period where the buoy measurements are unreasonably high.

2.4 WIND ~~toolkit~~Toolkit

The WTK was originally developed to support the next generation of wind integration studies with input from experts at NREL in production cost modelling and atmospheric science. In its core lies a large dataset calculated with the WRF model. The WRF model version 3.4.1 was used to create the meteorological data set, using ERA-Interim reanalysis data as inputs. The meteorological data set has a spatial resolution of 2x2 km and 5 min temporal resolution. It covers 7 years (2007–2013) and is available over the contiguous 48 US states, including the outer continental shelf. The WTK has been used by various research centers within NREL and by universities in multiple studies. A validation report is available for six onshore sites and three offshore sites (Draxl et al., 2015a). We will use the abbreviation WTK throughout this manuscript when referring to this particular dataset.

3 Methods

3.1 Synthetic aperture radar wind retrievals

SAR wind retrievals from the database of the Technical University of Denmark are used for this study and their processing is described in the following. SAR images are measures of the radar backscatter from the Earth's surface. The intensity of this backscatter is commonly referred to as the normalized radar cross section (NRCS). Level-1 SAR data are downloaded from the data providers and calibration is applied to obtain the ~~radar backscatter measured as the normalized radar cross section (NRCS).~~NRCS. The processing is done using the SAR Ocean Products System (SAROPS) software package (Monaldo et al., 2014). Radar backscatter ~~on~~and thus the NRCS of the ocean surface is determined by Bragg scattering (Valenzuela, 1978)~~ and~~ . This scattering mechanism is most sensitive to wave lengths on the ~~NRCS~~order of ~~the ocean surface~~10 cm. At this scale, waves can be ~~linked to a characteristic~~ assumed to be in local equilibrium with the wind speed ~~using a geophysical model function~~and therefore, the NRCS and the wind speed are correlated. An empirical Geophysical Model Function (GMF~~).~~) can link the NRCS and additional radar parameters to the wind speed at 10 m height above the sea surface.

For C-band radars, the C-band Model (CMOD)-family of functions is most widely used and CMOD5.N~~ is used for this study~~ (Hersbach, 2010)~~.~~ is chosen here for SAR wind retrievals. The ~~resulting~~retrieved wind speed is the equivalent neutral wind at 10 m above the ~~ocean~~sea surface. CMOD5.N is tuned for co-polarized vertical (VV) SAR observations and an incidence angle dependent polarization ratio is applied before processing co-polarized horizontal (HH) images (Mouche et al., 2005). For SAR wind retrievals, the wind direction needs to be known *a priori*. Wind directions are taken from global weather models from 10 ~~-~~m wind vectors and are interpolated spatially to match the SAR images. ~~Wind direction inputs~~Two sources of wind directions are used for the SAR wind retrieval~~ are obtained~~: until 2010, wind directions come from~~ ~~ the National Center for Atmospheric Research Climate Forecast System Reanalysis (CFSR) reanalysis data ~~are used until 2010~~ and from 2011 onwards, wind directions from the Global Forecast System (GFS) ~~data from 2011 onward.~~are used. The switch in wind direction input is present in the database of derived SAR wind maps due to a change to near real time processing.

Radarsat-1 was one of the early operational SAR systems and some of the ~~scenes are known to~~images have problematic distortions (Vachon et al., 1999); i.e., when stitching the subswaths together or there are issues with ~~correct~~the geolocation. These typically cause overestimated NRCS values and thus wind speeds that are too high. Because these problems are easy to detect visually but hard to formalize, Radarsat-1 data have been visually checked and problematic ~~scenes~~images are excluded. Additionally, NRCS values above 44° incidence angle are removed because of frequent unrealistically high NRCS values.

Formatted: Font: Italic

3.2 Merging synthetic aperture radar wind fields from different sensors

SAR~~-derived~~ wind speeds should correctly represent the wind conditions compared to in situ observations, but validation of SAR-derived wind speeds routinely leads to biases that are not consistent between studies (Christiansen et al., 2006; Horstmann et al., 2002; Lu et al., 2018; Takeyama et al., 2013). Deviations between studies can partially be explained by different GMFs that are used, but also by inconsistent calibration of the NRCS~~ values~~. Biases in the SAR~~-derived~~ wind speeds are problematic here because they translate to biases in the derived wind atlas. It is particularly problematic to have offsets in the biases between sensors, because these will introduce variability where spatial coverage of sensors changes over the study area. To date, SAR wind atlases have used a singular sensor or – if multiple sensors were merged – inherent differences have not been taken into account (Hasager et al., 2015; Karagali et al., 2018).

Badger et al. (2019) have found systematic differences in the bias when comparing wind speeds retrieved from Envisat and Sentinel-1A/B against in situ observations. Biases for Envisat showed a strong incidence angle dependency and ~~the~~a bias drift over the sensor's lifetime. Badger et al. (2019) found that these biases can be corrected~~.~~ through a calculation of NRCS ~~are calculated~~ from the modelled winds that are used for the SAR wind ~~speeds and compared~~inversion (see Section 2.4) followed by a comparison to the observed NRCS from the SAR~~ measurements~~. A linear fit of the NRCS differences depending on the incidence angle is then subtracted from the SAR ~~images~~observations before retrieving the SAR wind speeds. We apply the reported correction factors for Envisat and Sentinel-1A/B, which also account for the initial calibration problems of Sentinel-1A before 2015-11-25 (Miranda, 2015). Sentinel-1A data are split ~~in~~into two ~~time~~ periods~~,~~; before calibration (BC) and after calibration (AC). Corrections for Radarsat-1 are not available in Badger et al. (2019) and, therefore, we calculate adjustment factors from the available Radarsat-1 data using the same methodology. In accordance with recommendations from Badger et al. (2019), we exclude Envisat data acquired at incidence angles below 20°~~ have been excluded from the analysis~~ because of increased scatter and bias in the adjustment method.

3.2.1 Synthetic aperture radar ~~–~~**and** buoy comparisons

Comparisons between SAR and buoy measurements are conducted to confirm if results found in Badger et al. (2019) for Northern Europe are consistently present in this data set from the United States and whether the suggested adjustment method can remove biases between the sensors. Images during three ~~strong wind~~ storms ~~and~~with SAR wind speeds exceeding 30 m/s have been removed from the comparison because co-polarized SAR wind retrievals are expected to perform poorly in these conditions.

Comparisons between the wind speed from buoys and SAR need to account for inherent differences in the measurements. SAR images are matched with the closest buoy time stamp with a maximum difference of 30 minutes (Monaldo, 1988). SAR winds are instantaneous, and they are averaged spatially to a 3 km by 3 km cell to better match the temporal average of buoy measurements. Anemometers on buoys are typically mounted at heights between 3 and ~~5~~7 m while SAR winds are tuned to the height 10 m~~. Buoys~~ above the sea surface. Buoy wind speeds are therefore extrapolated to 10 m equivalent neutral ~~wind~~winds using the Coupled Ocean–Atmosphere Experiment COARE 3.0 algorithm ~~with~~using temperature measurements from the buoys (Fairall et al., 2003). In this algorithm, atmospheric stratification is described using the difference between the air and sea temperature together with empirically found constants. The wind speed is then extrapolated considering atmospheric stability and roughness as described by Charnock's relation (Charnock, 1955).

Figure 2 shows comparisons between SAR and buoys as scatter plots for SAR winds processed as described in Section 3.1. We call this 'default' processing as no inter-calibration of the SAR sensors is performed prior to wind retrieval processing. SAR wind speeds are split into 1 m/s bins according to the buoy wind speed. The SAR mean wind speed and standard deviation around this mean are calculated and plotted as well. Comparisons for all collocations in (a) show a slight bias for SAR to overestimate wind speeds by 0.30 m/s. The RMSE of 1.67 m/s is within the targets for satellite wind speed accuracies of 2 m/s (Figa-Saldaña et al., 2002). Distinguishing between sensors show that biases vary. Large biases towards overestimation of 0.62 and 0.82 m/s are respectively found in Envisat (b) and Sentinel-1A BC (e), while Radarsat-1 (c) is underestimating wind speeds by 0.89 m/s. Both Sentinel-1A AC (f) and Sentinel-1B (d) have neglectable biases. The results for Envisat and the two Sentinels are in line with ~~observations~~findings in Badger et al. (2019).

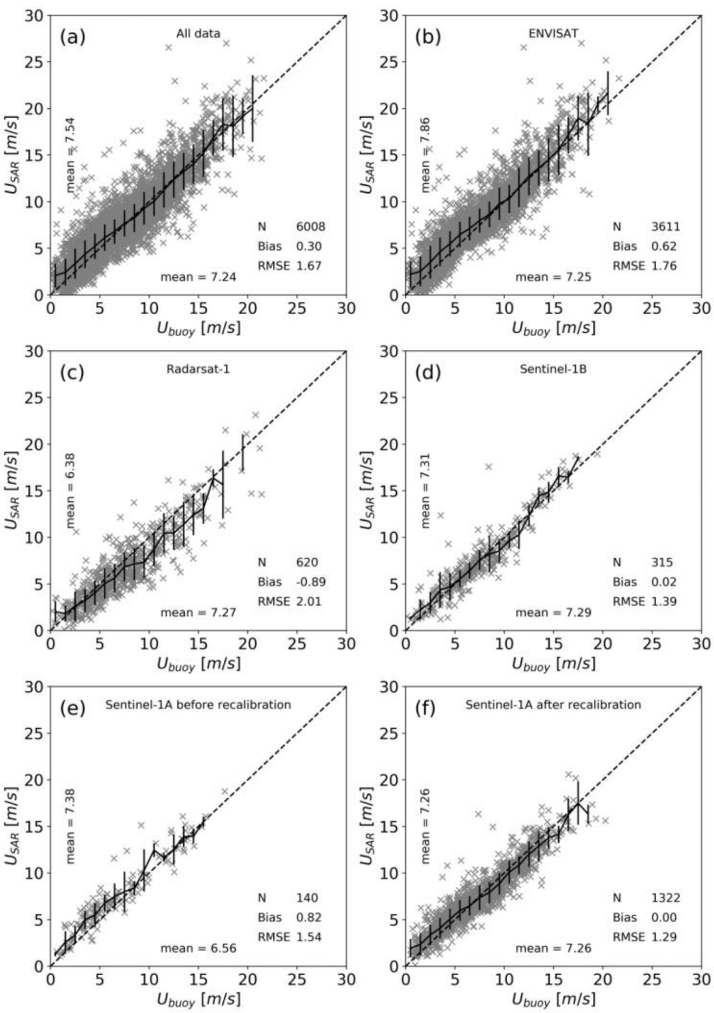

Figure 2: Scatter plots of SAR versus buoy winds at 10 m with default SAR wind processing for: (a) all data, (b) Envisat, (c) Radarsat-1, (d) Sentinel-1 BC, (e) Sentinel-~~1AC~~1 AC, and (f) Sentinel-1B. The black curves indicate the mean within each 1 m/s bin and the vertical lines around the mean value indicate one standard deviation within this bin.

Formatted: Caption, Line spacing: 1,5 lines

Figure 3 shows comparisons between SAR and buoy wind speeds after applying the intercalibration process described in Section 3.2. ~~Comparisons~~Results for ~~data from~~ all satellites have improved ~~both~~ in terms of a change of the bias from 0.30 to -0.04 m/s and of the RMSE from 1.67 to 1.46 m/s. Considering each of the sensors separately, biases lie between -0.2 and 0.03 m/s, which is a drastic improvement compared to biases in Figure 2 ranging between -0.89 to 0.82 m/s. Large improvements are found for Envisat, Radarsat-1, and Sentinel-~~1~~1A BC both in terms of biases and RMSE. ~~Closely examining the~~ The two largest data sets, Envisat (b) and Sentinel-1A AC (e), ~~an overestimation of~~show a higher mean wind speed from SAR when the buoy wind speed is less than 7 m/s and ~~an underestimation of more than~~vice versa lower mean wind speeds from SAR when buoy wind speeds exceed 9 m/s ~~can be observed. These~~. For Envisat, these opposing biases are averaged to nearly zero in the overall bias. ~~The~~Altogether, the intercalibrated SAR winds have smaller biases than the individual data sets and small differences between the sensors compared to the default processing. The following analysis will therefore be based on ~~these adjusted~~the intercalibrated SAR wind maps.

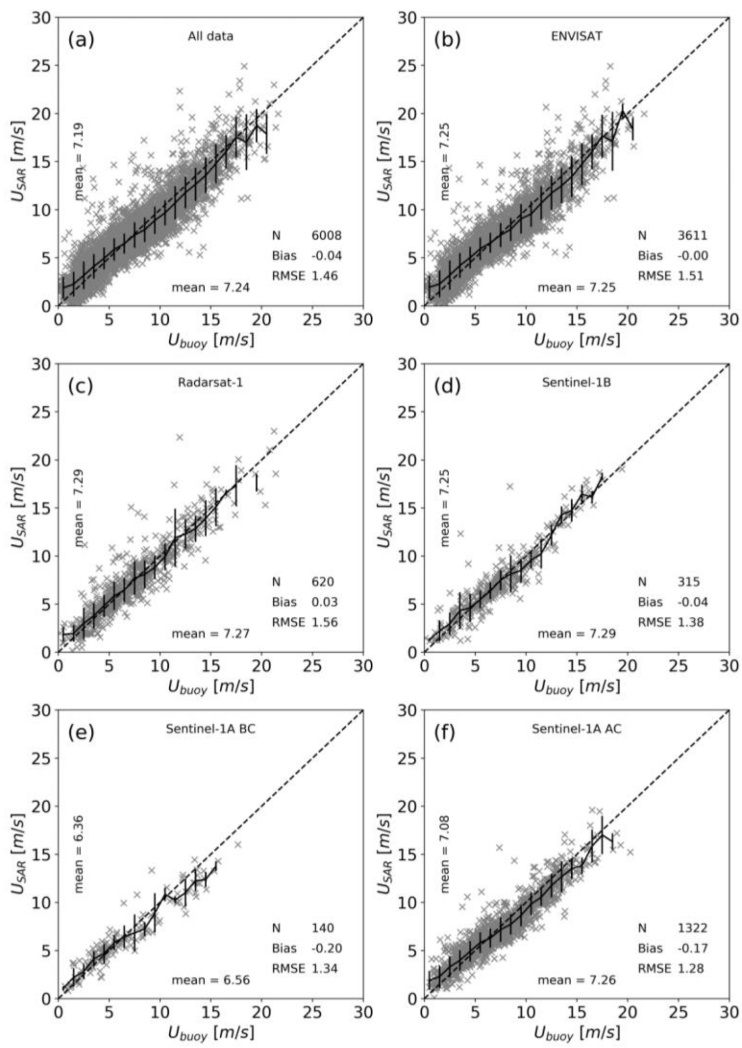
(a)
All data
N 6008
Bias -0.04
RMSE 1.46
mean = 7.24
mean = 7.19
(b)
ENVISAT
N 3611
Bias -0.00
RMSE 1.51
mean = 7.25
mean = 7.25
(c)
Radarsat-1
N 620
Bias 0.03
RMSE 1.56
mean = 7.27
mean = 7.29
(d)
Sentinel-1B
N 315
Bias -0.04
RMSE 1.38
mean = 7.29
mean = 7.25
(e)
Sentinel-1A BC
N 140
Bias -0.20
RMSE 1.34
mean = 6.56
mean = 6.36
(f)
Sentinel-1A AC
N 1322
Bias -0.17
RMSE 1.28
mean = 7.26
mean = 7.08
U_{buoy} $[m/s]$
U_{SAR} $[m/s]$

Figure 3: Scatter plots of intercalibrated SAR versus buoy winds at 10 m ~~with incidence angle adjusted processing~~ for: (a) all data, (b) Envisat, (c) Radarsat-1, (d) Sentinel-~~1~~1A BC, (e) Sentinel-~~1AC~~1A AC, and (f) Sentinel-1B. The black curves indicate the mean within each 1 m/s bin and the vertical lines around the mean value indicate one standard deviation within this bin.

Formatted: Caption

3.3 SAR wind atlas methods

A wind atlas is a map of statistical representations of the wind speed over a designated area. The wind climate is typically represented by a Weibull distribution of wind observations that is characterized by the Weibull scale parameter (A [m/s]) and ~~the~~a shape parameter (k [unitless]). They are related to the mean energy density (E [W/m^2]) by:

$$E = \frac{1}{2}\rho A^3 \Gamma\left(1 + \frac{3}{k}\right) \quad (1)$$

where ρ is the air density, and Γ the Gamma function. ~~The mean wind speed can be defined as the arithmetic mean of the available samples.~~

$$\cancel{U = \frac{1}{F}\sum_n u_n \quad (2)}$$

~~With the wind speed of the individual image u_n and the total number of observations F.~~

A typical approach in wind energy is to use the Wind Atlas Analysis and Application (WAsP) program that implements methods from the first European ~~wind atlas~~Wind Atlas (Troen and Petersen, 1989). Wind atlases are normally generated ~~by taking the mean wind speed~~ from long time series, but it is also possible to use the quasi-instantaneous wind fields derived from SAR (Christiansen et al., 2006). ~~Properties of the~~A special version of WAsP developed for satellite-based inputs (S-WAsP) is used here. The ~~acquisition such as temporally fixed overpasses, relatively low sampling, and data truncation lead to uncertainty in a SAR-based wind atlas (Barthelmie and Pryor, 2003). A special version of WAsP developed for satellite-based wind atlases (S-WAsP) is used in this study.~~ Weibull fitting uses 2nd moments as recommended in Pryor et al. (2003). SAR wind ~~scenes~~images are ~~averaged~~projected on a regular WGS84 grid with 0.02° cell spacing before processing the data to a wind atlas. The mean wind speed can be defined as the arithmetic mean of the available samples.

$$U = \frac{1}{F}\sum_n u_n \quad (2)$$

With the wind speed of the individual image u_n averaged on the 0.02° grid and the total number of observations F.

Results from a SAR-based wind atlas can be noisy because of the high resolution of wind fields and the relatively few samples. Therefore, we apply a Gaussian filter using a standard deviation of 0.03° with a cutoff at 0.06° to smooth the mean wind fields. Properties of the satellite data acquisition such as temporally fixed overpasses, relatively low sampling, and data truncation lead to uncertainty in a SAR-based wind atlas (Barthelmie and Pryor, 2003). ~~Sensors acquire images at fixed times of day, which will can cause a bias in the mean wind speed where diurnal cycles are present. Advanced methods for classifying SAR wind maps are available (Badger et al., 2010). We chose~~Advanced methods for classifying SAR wind maps are available (Badger et al., 2010) but we choose to apply random sampling considering all images available, which is recommended where more than 400 images are available (Pryor et al., 2003). This approach is also used in earlier SAR-based wind atlases (Hasager et al., 2011). The influence of diurnal cycles is investigated in more detail in Section 4.1.1.

SAR ~~scenes are~~images may be acquired ~~primarily~~ for other purposes ~~other~~ than wind resource assessment~~. This~~, e.g. sea ice monitoring, and this can influence the temporal coverage of acquisitions. ~~One example is sea~~Sea ice detection ~~that~~ will mainly occur during the winter months (Sandven et al., 1999). The study domain is located in the mid-latitudes and winds are expected to change with the seasons. We therefore check for seasonal biases in the data acquisition~~, described in~~ (see also Section 4.1.2~~.~~). For the arithmetic mean wind speed in Eq. 2, the seasonal bias can be corrected by calculating mean wind speeds U_m by month (Monaldo, 2011):

$$U_m = \frac{1}{F_m} \sum_n u_{n,m} \quad (3)$$

with the number of observations F_m for each month m and $u_{n,m}$ the SAR wind speeds occurring in this month. Monthly mean wind speeds are then averaged to a seasonally corrected mean wind speed U_{sc}:

$$U_{sc} = \sum_m \frac{F_m}{F} U_m \quad (4)$$

S-WAsP is not able to account for seasonal biases in the Weibull parameter estimation. Therefore, no seasonally corrected Weibull parameters or energy densities are available.

4 Results

4.1 Wind resource statistics

In the following, we present the first ~~SAR-based~~ wind atlas for the US East Coast based on intercalibrated SAR wind fields from four ~~systems~~different sensors. Figure 4 shows wind statistics at 10 m: (a) The arithmetic mean wind speed from Eq. 2 calculated from SAR and (b) the mean wind speed from modelled data (WTK). A visual comparison shows similar features. WTK wind speed contours are smoother than those from SAR for two reasons: i) SAR~~-derived~~ wind speeds are based on high ~~-~~resolution ~~observation~~observations that can resolve sub-kilometer scale ~~variation~~variationa in the wind fields, and ii) SAR-derived mean winds are derived from fewer samples while WTK are based on 7 full years of hourly modelled wind speeds. Wind speeds are lower close to the coast and increase with the distance from shore~~.~~ for both SAR and WTK. A band of high winds is located off the coast of North Carolina and extends to the northwest with higher mean wind speeds in SAR than in the WTK. Horizontal variations of the SAR wind speed are higher than for WTK. The mean wind speeds are lower for SAR than WTK in a region close to the shores of Virginia and Delaware. Another clear difference is the wind speed in the Gulf of Maine. WTK data show ~~winds of~~mean wind speeds less than 7.5 m/s while SAR winds go up to 8.5 m/s. In both data sets, a feature of lower mean wind speed is present to the southeast of Nantucket but more pronounced in the SAR-derived map.

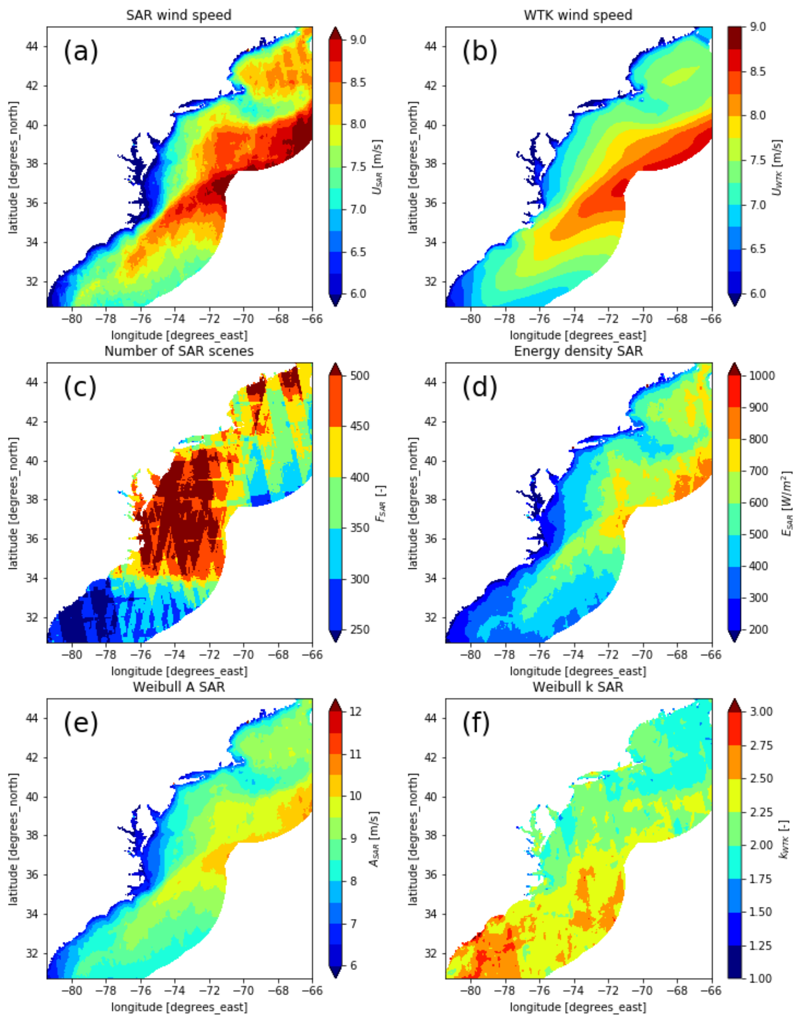
SAR wind speed
(a)
WTK wind speed
(b)
Number of SAR scenes
(c)
Energy density SAR
(d)
Weibull A SAR
(e)
Weibull k SAR
(f)
latitude [degrees_north]
longitude [degrees_east]
U_{SAR} [m/s]
U_{WTK} [m/s]
F_{SAR} [-]
E_{SAR} [W/m^2]
A_{SAR} [m/s]
k_{WTK} [-]

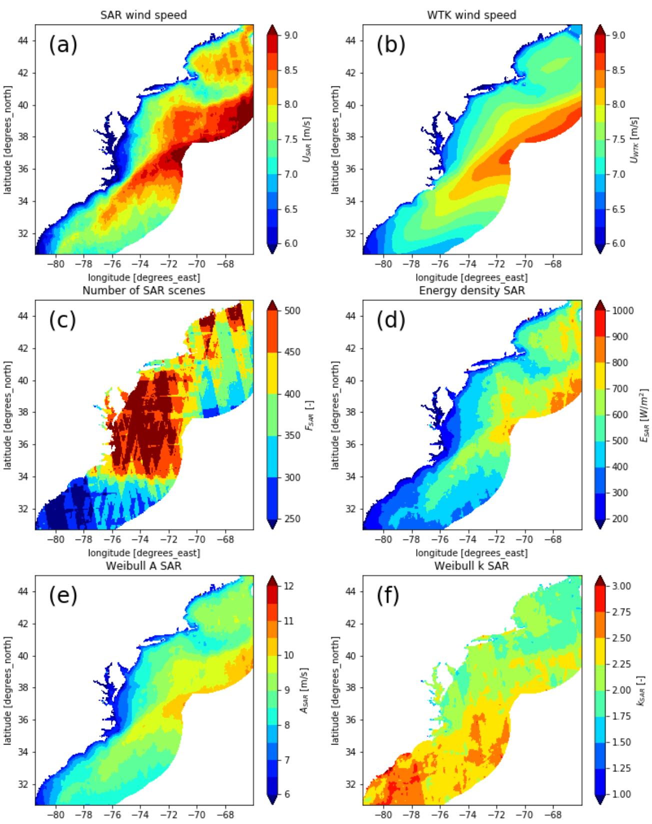

Figure 4: Wind atlas ~~maps~~ at 10 m ~~for~~above sea level: (a) arithmetic mean wind speed from SAR ~~wind speed~~, (b) mean wind speed from ~~WIND toolkit~~WTK, (c) number of SAR samples, (d) SAR energy density; (e) SAR Weibull scale parameter A; (f) SAR Weibull shape parameter.

North of 34° latitude, more than 350 samples are used, but fewer than 250 are used off the coast of Georgia (Fig. 4c). The energy density ranges from 200 W/m^2 close to shore to 800 W/m^2 far offshore (Fig. 4d). The Weibull shape parameter A (Figure 4e) shows similar features as the wind speeds and the energy density. The scale parameter, k (Figure 4e) ranges between 2 and 3 in the south and 1.75 and 2.5 in the north of the domain. High k values are associated with a narrow Weibull wind speed distribution.

Wind resources and wind roses are compared between SAR, WTK, and in situ buoy measurements for three example locations along the coast in Figure 5. Buoy 44029 is located in the Gulf of Maine, buoy 44009 is located off the Delaware coast, and buoy 41038 is located off North Carolina; see Figure 1 for detailed positions. Buoy data are filtered to cover full years (at least 80% available data) to avoid seasonal sampling biases~~; between~~. Between 7 and 10 years of measurements are available at the buoy locations. WTK covers 7 full years and the SAR winds are sampled over the entire period from 1998 to 2018 but less frequently. SAR wind speeds are expressed as equivalent neutral ~~wind~~winds while the 10 m wind speeds from WTK are stability-dependent wind speeds. Buoy wind speeds are extrapolated accordingly but stability effects are small (less than 0.2 m/s differences for the mean wind speed).

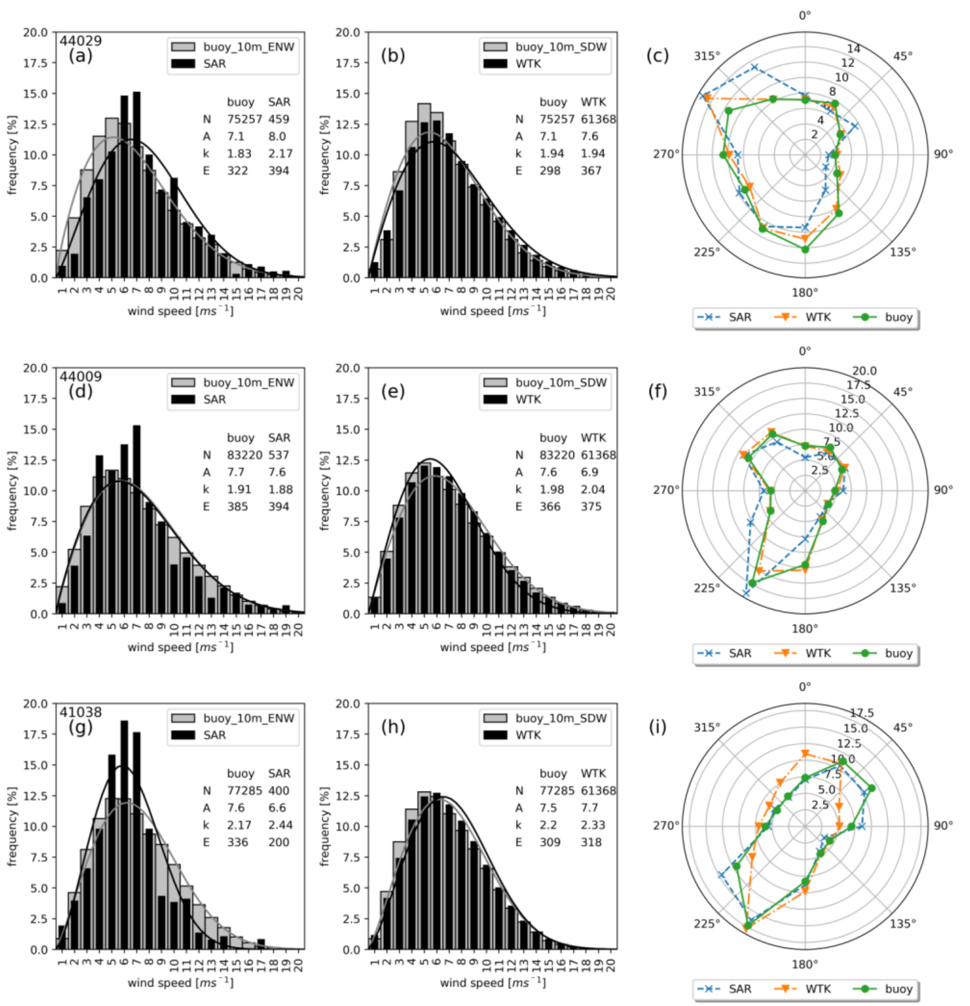

Figure 5: Weibull fits and wind roses for buoys 44029 (a-c), 44009 (d-f), and 41038 (g-i). SAR on the left (a,d,g), ~~WIND toolkit~~WTK in the middle (b,e,h), and wind roses for buoy, SAR, and ~~WIND toolkit~~WTK on the right (c,f,i). Key characteristics are given in the tables: Number of observations (N), Weibull shape (A~~),~~,) in m/s, Weibull scale (~~E). Units of~~k), and the ~~tables are: [N] = --, [A] = m/s, [k] = --, [E] =~~energy density (E) in W/m^2.

SAR-based results show good agreement at buoy 44009 but distributions are skewed towards higher wind speeds at 44029 and lower at 41038, while WTK distributions generally agree well with the buoy data. Wind directions for SAR show more winds from the northwest for buoy 44029 and agree well with buoy data otherwise. Wind directions from the WTK show most deviations for buoy 41038. There are large deviations ranging from -136 to 72 W/m^2 between wind resources as measured from buoys and SAR that merit closer investigation in the following.

4.1.1 Diurnal cycle

As noted in Section 3.3, SAR sensors acquire data at fixed times of the day. We investigate influences of this ~~might have~~ on the wind retrieval by investigating the diurnal cycle at five buoys located across the study domain. In addition to the three buoys in Figure 5, buoy 44065 is located south of New York City and 44072 is in Chesapeake Bay. All buoys are within 20 km of ~~shore~~the shoreline with the exception of buoy 44009, which is located approximately 60 km offshore. The ~~shape of the~~ diurnal variation of the mean wind speed is similar between these buoys with minima between 10 am and 12 pm local time; see Figure 6. Buoy 44009 shows less diurnal variation, which might be ~~connected~~due to ~~this~~the buoy ~~being located~~location further offshore. Overlaid in Fig. 6 is a histogram of the satellite acquisition times showing that ~~scenes~~images are not randomly sampled ~~as expected from~~due to the polar ~~orbit.~~orbits of satellites. We note that the ~~afternoon~~morning times of ENV ~~overpass~~overpasses coincide with ~~a minimum~~the minima in the ~~diurnal variation~~mean wind speeds, while S1A, S1B, and RS1 overpasses are outside this time interval.

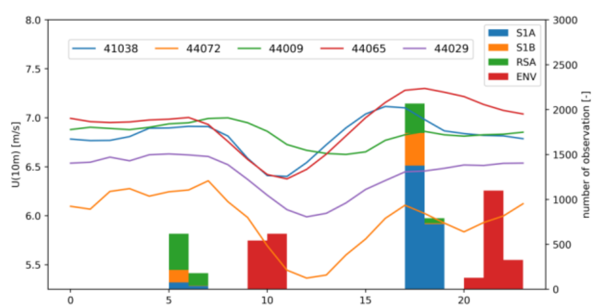

Figure 6: Mean wind speed of selected buoys in local time (UTC – 5). The bars indicate the number of satellite observations for Radarsat (RSA), Envisat (ENV), Sentinel-1A (S1A), and Sentinel-1B (S1B).

4.1.2 Seasonal sampling bias

We investigate seasonal sampling biases in SAR for four regions of 2° by 2° along the ~~coast.~~US East Coast. Figure 7 shows the spatial average of monthly acquisition frequency F_m/F and monthly mean wind speed U_m from Eq. 3 and 4 at four areas. Acquisitions are unevenly distributed over the year. More data are available ~~in~~during the winter in the Gulf of Maine while

Delaware and North Carolina are biased towards late summer to early autumn. U_m shows considerable seasonal changes with generally lower winds in summer and higher winds in winter.

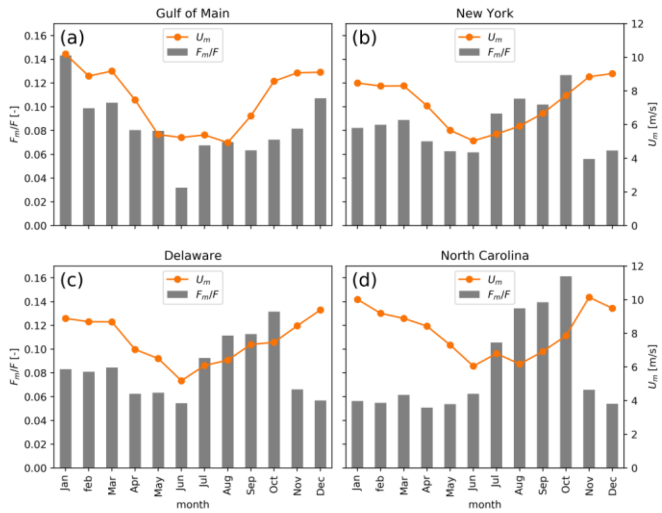

Gulf of Main
New York
Delaware
North Carolina
(a)
(b)
(c)
(d)
U_m
F_m/F
F_m/F [-]
U_m [m/s]
Jan
feb
Mar
Apr
May
Jun
Jul
Aug
Sep
Oct
Nov
Dec
month

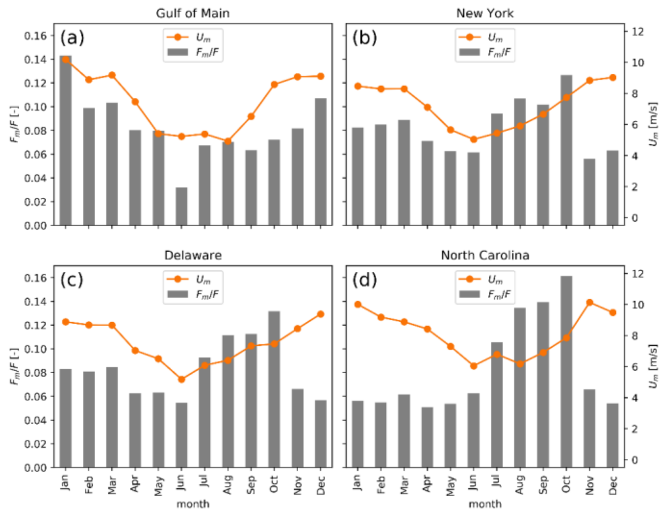

Figure 7: Frequency of data acquisition (Fm/F) and mean SAR wind speeds (Um) averaged by month over four regions close to: (a) Gulf of Maine, (b) New York, (c) Delaware, (d) North Carolina

Figure 7 shows considerable seasonal sampling biases. A seasonally corrected SAR (SAR_SC) mean wind speed map is calculated from Eq. 4 and shown in Figure 8a together with the differences with respect to uncorrected maps from Fig. 8b. ~~Seasonal~~The seasonal correction reduces wind speeds in the north, while it increases wind speeds in the south of the study domain.

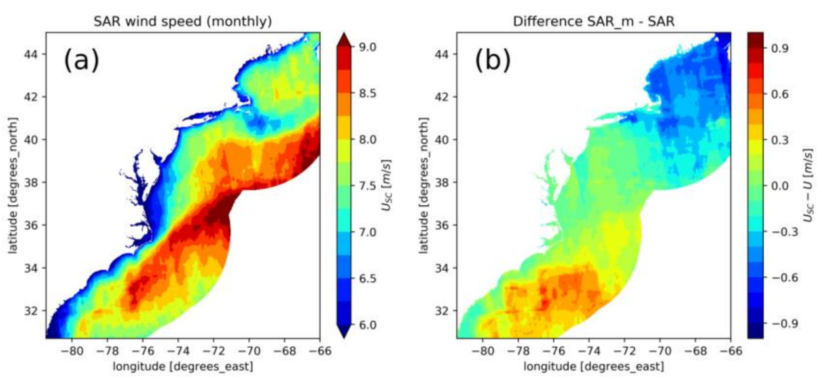

Figure 8: (a) Seasonally corrected SAR wind speed (b) difference between seasonally corrected and original SAR map.

Two SAR-based mean wind speed maps in Figure 4a and Figure 8a have been calculated. The one better representing the long-term wind conditions is determined from comparison to long-term mean wind speeds from the ocean buoys. Buoys are required to have at least 7 full years (more than 80% recovery rate) of measurements. It is necessary to use a representative position for the buoys because buoy positions can change over time and SAR or WTK are not collocated in time. This requires that buoy positions do not change significantly during the measurement period. Buoy 41002 and 44018 are removed because their location changes more than 100 km. Sixteen buoys fulfil these criteria and statistics on comparisons to the SAR mean wind speed in Figure 4a, WTK mean wind speed in Figure 4b, and the seasonally corrected SAR mean wind speed in Figure 8 are presented in Table 1.

Table 2: Mean absolute error (MAE), root mean square error (RMSE), and bias between mean wind speeds from buoys ~~as well as~~versus SAR ~~(U),~~, seasonally corrected SAR (~~U_{SC}),~~SAR_SC), and WTK.

	MEA	RMSE	Bias
SAR	0.51	0.63	0.34
SAR_SC	0.3	0.39	0.09
WTK	0.24	0.30	0.15

Formatted Table

The seasonally corrected mean wind speed ~~U_{SC}~~ from SAR (SAR_SC) shows a lower RMSE, MAE, and bias~~.~~ than the uncorrected SAR data set. We consider ~~this to be~~SAR_SC a better representation of the seasonality~~. U_{SC}~~ and it will therefore be used for comparisons with the WTK in Section 4.2.

4.2 Spatial wind variability from SAR and WTK

To compare SAR_SC and WTK mean wind speeds in the coastal zone, we define transects perpendicular to the generalized coastline of the United States up to 100 km from ~~shore.~~the shoreline. Because of the complexity of the shoreline, a compromise needs to be found between perpendicular transects, avoiding crossing transects, and the definition of distance to shore for convex corners. The resulting transects are shown in Figure 9 and are labelled with unique identifiers (transect_id) ranging from 0 in the north to 650 in the south.

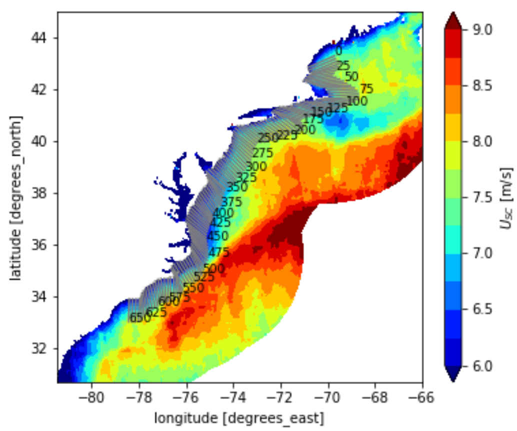

Figure 9: Seasonally corrected SAR mean wind speed maps (SAR_SC) with transects perpendicular to shore (every fifth transect is plotted). Starting at transect_id 0 in the Gulf of Maine going to transect_id 650 off North Carolina.

Wind speeds are linearly interpolated along each transect every 2 km. Figure 10 shows the wind speeds per transect ID and as a function of distance to shore. These plots can be seen as a horizontal sheet of mean wind speeds along the coastline perpendicular and parallel to shore. The white areas are land contamination in SAR wind maps originating from islands not accounted for in the generalized coastline. Again, we can see similarities in the features on large scales with a band of high wind speed between transect_id 500 and 600 but also smaller features like an increased wind speed at the mouth of the Delaware River around transect_id 350.

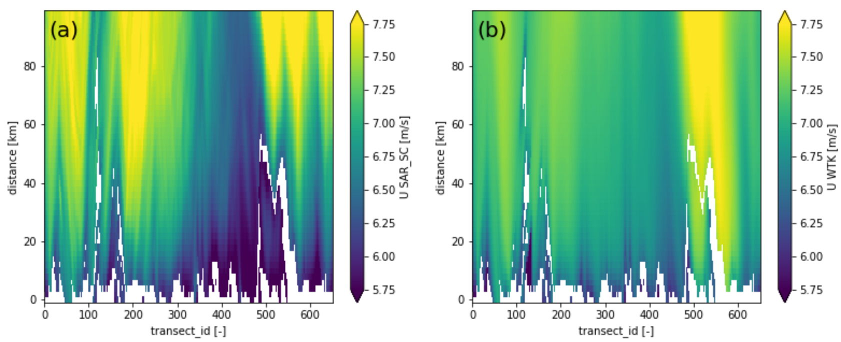

Figure 10: ~~Wind~~Mean wind speeds at 10 m ~~over~~above sea level for all transects as a function of the distance to shore. (a) SAR ~~wind speed seasonally corrected~~_SC, (b) ~~WIND toolkit~~WTK.

The presentation of wind speeds in Figure 10 represents spatial structures of the mean winds along the coast but it is hard to assess differences visually. We will focus on wind speed variations in two directions: along-shore and perpendicular to the coastline. The latter is commonly referred to as a coastal wind speed gradient.

4.2.1 Along-shore variation

Figure 11 shows wind speed transects along the shore averaged over distances to shore of [10,20], [20,30], [40,60], and [60,100] km. From transect_id 0 to 300 the two transects closest to shore (Fig. 11 a and b) show remarkably good agreement, both absolute and in shape. Further offshore, in panels (c) and (d), the positions of local maxima and minima are similar but the amplitude of these features is larger for SAR_SC than ~~WRF~~WTK. From transect_id 300 onward (southward), SAR_SC gives consistently lower wind speeds with the exception in panel (d) around transect_id 570 and 650.

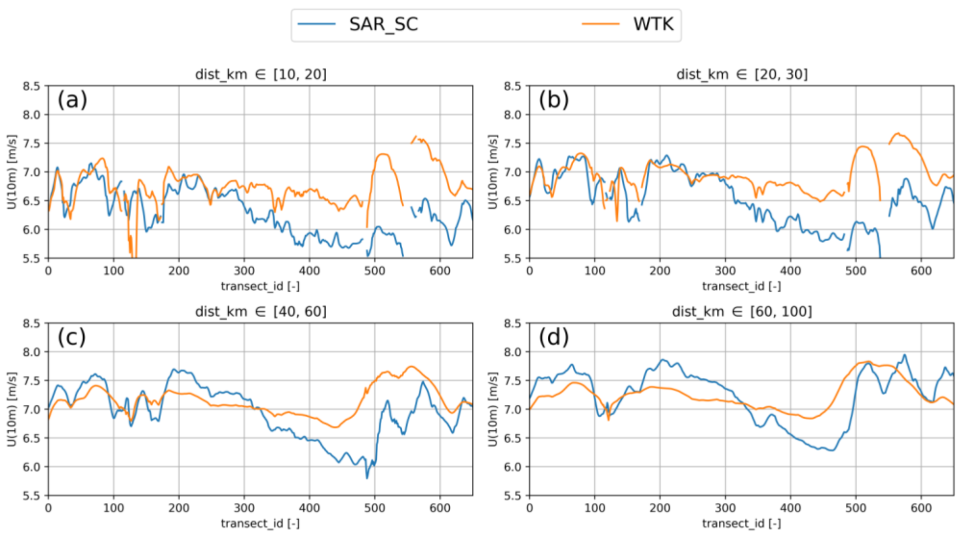

Figure 11: Along-shore variation of the mean wind speeds for distance to shore intervals of: (a) [10,20], (b) [20,30], (c) [40,60], and (d) [60,100] km.

The region closer than 60 km to shore is most interesting for wind farm development. Here, SAR observations suggest high wind speeds in the north up to transect_id 250, while WTK consistently shows higher wind from transect_id 500 southward.

4.2.2 Coastal gradients

Wind speeds averaged over the distance to shore for six regions are shown in Figure 12. All regions show coastal gradients with the typical increase in mean wind speed with distance from ~~shore.~~the shoreline. For Fig. 12a, around Nantucket, there is very good agreement both in the gradient and in the absolute value. Regions (b), (c), and (f) show similar ~~behavior~~behaviours, with SAR_SC exhibiting lower wind speeds closer to shore but higher gradients resulting in higher ~~SAR winds~~wind speeds further offshore. Gradients are similar for (d) but SAR_SC winds are offset by 0.7 m/s toward lower wind speeds. The most pronounced differences in terms of wind speed gradients are found around Pamlico Sound (e) with SAR_SC winds up to 1.5 m/s lower close to shore and a steep gradient from 40 to 100 km offshore.

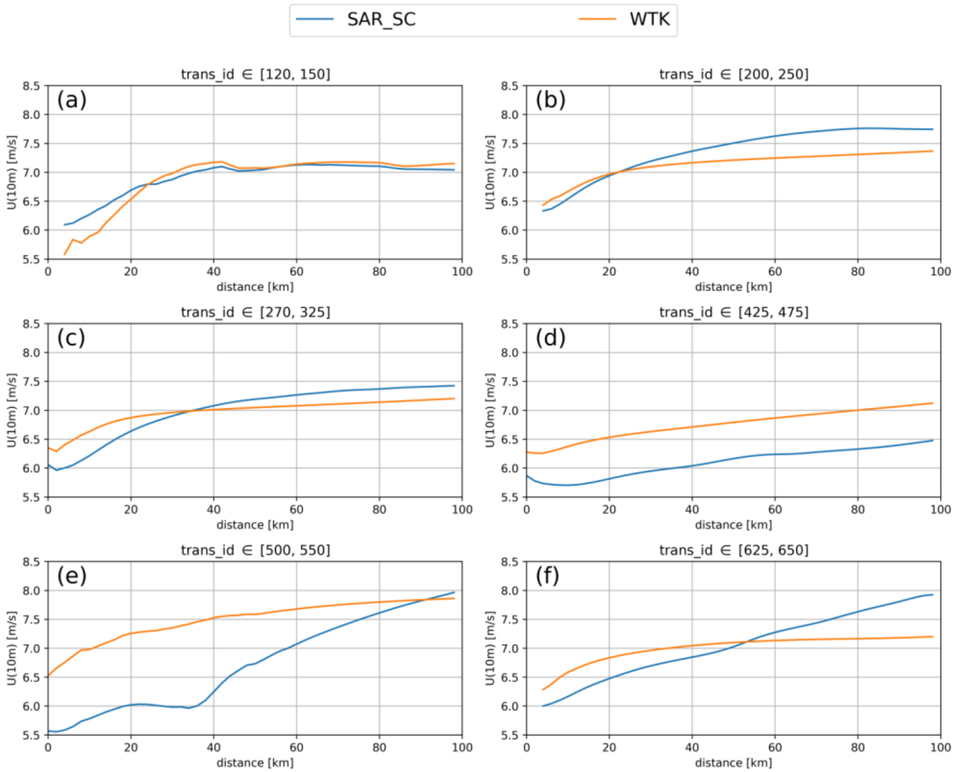

Figure 12: Mean wind speeds averaged over several transects covering six different regions. From north to south (a) Nantucket, (b) Long Island, (c) State of New York, (d) Virginia to Delaware, (e) Pamlico Sound, (f) southern part of North Carolina.

The transects show consistently higher wind speed gradients with the exception of the most northern region around Nantucket (Figure 12a). The wind speed gradient is defined as:

$$grad = \frac{dU}{dx}$$

where U is the mean wind speed and x is the distance to shore. The wind speed gradient is averaged for each transect resulting in 650 mean gradients for SAR_SC and WTK. A distribution thesis is shown in Figure 13. Mean gradients are mostly positive, indicating higher wind speeds further offshore as expected. For WTK, the distribution is almost symmetric with a mean of

0.91 m/s per 100 km. The distribution from SAR SC is more skewed and clearly separated from the WTK. The mean of the distribution is 1.40 m/s per 100 km, which is considerably higher than for the WTK ~~-~~.

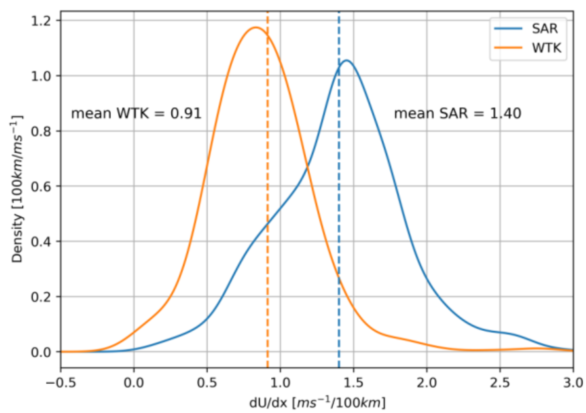

Figure 13: Density plot of wind speed gradients from SAR and ~~WIND toolkit~~WTK. Dashed lines indicate the mean values.

4.2.3 Wind resource variation within Bureau of Offshore Energy Management areas

Wind farm development is allowed within the limits of the offshore lease areas defined by the BOEM; see Figure 14. Because lease areas are typically several hundred square kilometers large, wind resources are expected to vary within each of the areas. Information on the magnitude of this variation is needed for wind farm development.

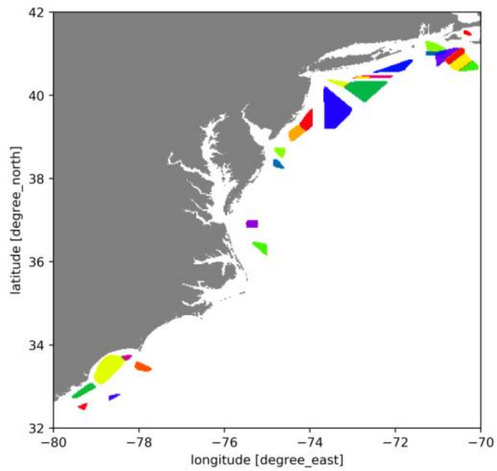

Figure 14: Bureau of Offshore Energy Management lease areas for the US East Coast. Color codes are used to differentiate different areas.

We select mean wind speeds from SAR_SC and the WTK at all grid points within a given lease area. The distribution of mean wind speeds within each area is then calculated and presented as a violin plot in Figure 15. The variation of mean wind speeds is higher from SAR for all areas except Cape Wind and Kitty Hawk. The average of the differences between minimum and maximum are 0.2 m/s for the WTK and 0.47 m/s from SAR_SC. This indicates that the WTK predicts much less variation of wind resources within a potential wind farm site than SAR_SC. Note that a mesoscale numerical weather prediction model, such as ~~WRF~~the model behind WTK, is unable to pick up wind speed variations in the order of 0.5 m/s, and their RMSEs are typically more than 0.5 m/s.

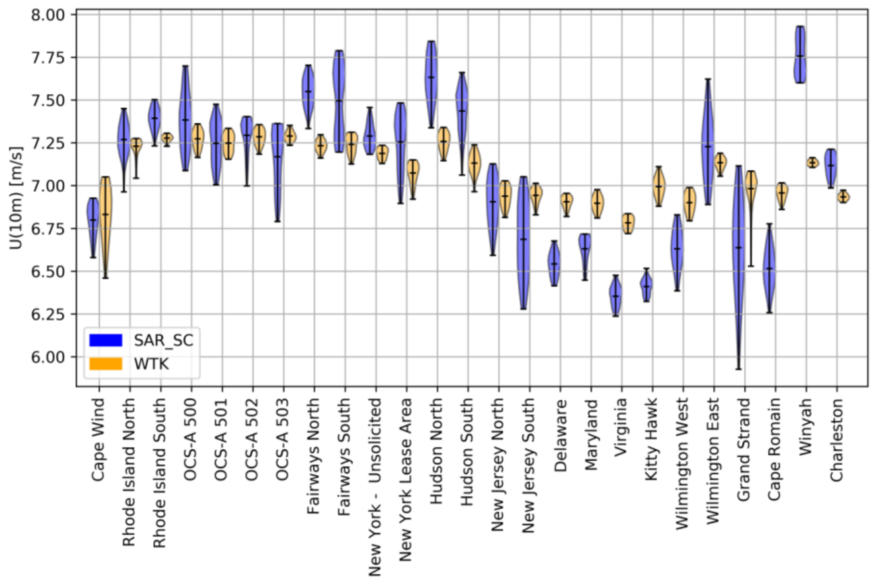

Figure 15: Violin plot for wind speeds from seasonally corrected SAR and ~~WIND toolkit~~WTK. Potential lease sites are ordered from north (left) to south (right).

5 Discussion

In the following, we discuss the results from the evaluation of the SAR wind atlas and the associated artefacts from the sampling. The representation of wind speed variations in the coastal zone is discussed as ~~measured~~retrieved from SAR and modelled in the WTK.

a) Validation of intercalibrated SAR wind archive with buoys

This study presents the first SAR wind atlas merging archives from four sensors into a consistent data set. Extensive comparisons with buoys show that even though data are processed consistently with CMOD5.N, biases between the sensors range from -0.89 to 0.62 m/s (see Figure 1), which is similar to results from northern Europe. Badger et al. (2019) suggested intercalibration to remove biases by adjusting the NRCS as a linear function of the incidence angle using modelled wind speed and direction inputs. Those adjustments decrease the difference in biases between sensors to 0.2 m/s. Overall, a tendency to overestimation for low wind speeds and underestimation for high wind speeds remains in the SAR wind maps, which influences the Weibull fitting~~.~~ performed here. Two findings speak ~~to~~for the generality of this approach: i) Intercalibration tables derived over northern Europe can be applied for the US East Coast; ii) applying the suggested intercalibration method to Radarsat-1 data reduces the bias to 0.03 m/s. ~~This concept~~The intercalibration should in no way substitute efforts to better understand scattering mechanisms ~~that~~on order to improve the calibration of NRCS as well as GMFs for wind retrieval (Troitskaya et al., 2018). Tuning NRCS values is an application-driven approach, which is necessary at present in order to produce wind maps with consistently low ~~bias~~biases. This ~~is in contrast to~~approach is significantly different from previous and current efforts to determine the most suitable GMF for SAR wind retrievals (Christiansen et al., 2006; Takeyama et al., 2013).

b) SAR wind atlas for the US East Coast

We have produced a SAR-based wind atlas of the US East Coast covering the coast from Georgia to the Canadian border. An alternative to SAR measurements are scatterometers (Stoffelen and Anderson, 1997). From a wind resource perspective, their main advantage is the higher temporal resolution, but it comes at the cost of a lower spatial resolution of typically 25 km. Merging SAR and scatterometer wind data to create a wind atlas has been done (Hasager et al., 2015), but this approach needs further refinement to fully utilize the high temporal coverage from scatterometers and the high spatial resolution from SAR.
~~The~~We have estimated the Weibull parameters A and k, energy ~~density~~densities, and mean wind speeds ~~are calculated~~ from all the available SAR wind maps; see Figure 4. The energy density, Weibull shape (A~~,~~), and mean wind speed generally increase with the distance from shore. The Weibull scale parameter (k) is high in the south and lower in the north. The Weibull k parameter requires more samples than wind speed or shape parameter to be correctly estimated (Barthelmie and Pryor, 2003). The area with high shape parameters coincides with a low number of samples and significant seasonal ~~bias~~biases in the sampling, which casts doubt on the accuracy of results in these instances.
For the purpose of comparing the SAR-based wind atlas to the WTK, it is desirable to keep the SAR data as independent from modelling results as possible. Therefore, we have not utilized any information from the WTK data set to perform stability correction of the SAR winds. The buoy observations used in this analysis indicate that for heights of 10 m or less above the sea surface, atmospheric stability effects on the wind speed are smaller than 0.2 m/s on average. It is however possible that larger deviations from the neutral wind profile occur for specific instances.
The presented SAR wind atlas is calculated at a 10 m height~~; however~~ above the sea surface. However, for wind energy applications, estimates closer to turbine hub heights at 100 m or higher above sea level would be more desirable. Extrapolation of the wind atlas results presented here is possible using model-derived stability ~~inputs~~corrections to the long-term average wind profile (Badger et al., 2016). ~~For~~ The extrapolation would first require a careful validation of the ~~purpose of comparing the wind atlas to the WTK, it is desirable to have the SAR data as independent from modelling results as possible. Extrapolating these results~~model outputs against bouy observations and is therefore beyond the scope of this study~~ but~~. The vertical extrapolation would increase the applicability of the SAR-derived wind speeds for wind energy purposes and will be

considered in the future. ~~Comparisons~~Our wind atlas and comparisons at the 10~~-~~m ~~are nonetheless~~level represent a valuable ~~to~~first step, which helps us assess differences ~~relative to mesoscale models and to gain~~between data sets and gaining insight in the horizontal variation of wind resources.

c) Wind resource comparisons

This study shows a comparison between SAR and WTK, assuming that both are representative for the wind climatology. A method to sample SAR winds according to wind classes based on modelled climatology is available to reduce the number of samples necessary for wind resource assessment (Badger et al., 2010). This has the advantage of choosing ~~scenes~~SAR images that are more representative for the large-scale wind conditions but comes with the disadvantage of weakening the independence of the SAR-derived results. Combining data with other in situ observations as done in Doubrawa et al. (2015) is an option, but the density of measurements on the US East Coast is lower than in the Great Lakes, where the method was developed.

SAR-derived wind resources overestimate the energy density by 72 W/m^2 at buoy 44029 and underestimate them by 136 W/m^2 for buoy 41038. Sampling of the SAR ~~scenes~~images shows considerably uneven sampling between different seasons (Figure 7). In the region of buoy 44029, the winter months with high wind speeds are overrepresented. Wind resource estimates derived from these data will retain a bias to higher wind speeds and thus overestimate the wind resource, which is in line with our observations. For buoy 41038, an opposing bias towards summer and early autumn associated with low wind speeds could explain the underestimation of wind resources. The resource estimate from SAR shows little difference in Weibull parameters and the energy density for buoy 44009. In this region, seasonal sampling is more evenly distributed and oversampling occurs between the extrema. Wind resource estimates from the WTK have been made at the same buoy locations. Generally, the wind resources are estimated more accurately than from SAR but overestimations of 69 W/m^2 occur at buoy 44029.

SAR wind atlases for other regions have generally not reported seasonal dependency in the data coverage (Hasager et al., 2011; Karagali et al., 2014). ~~A~~We have implemented a simple method to overcome this problem~~ was implemented~~ using weighted monthly averages to calculate the mean wind speed (Eq. 4) (Monaldo, 2011). This seasonally corrected mean reduces wind speeds in the north, while increasing them in the south of the study domain. Differences frequently exceed 0.5 m/s, which are substantial for a product that should be used in the context of wind energy. The seasonally corrected mean wind agrees better with long-term means from buoy ~~observation~~observations (Table 2), both in terms of mean errors and RMSE, and we ~~see~~consider them ~~to be the~~a better choice when estimating a wind climatology. Using monthly weights in the estimation of SAR-derived Weibull parameters should be possible but implementing and validating such a method is beyond the scope of this article.

d) Influences of diurnal variability

SAR satellites operate on orbits with fixed times for ascending and descending tracks 12 hours apart. This sampling ~~bias~~pattern influences results in ~~the~~our wind atlas. The time of day of the observations from Envisat are approximately 10 am and 10 pm, while Sentinel-1A~~, 1B~~/B, and Radarsat-1 are observing ~~at~~around 5 am and 5 pm local time. Envisat contributes the most observations in this study and thus its temporal bias will largely influence results. For buoy 44072 located in the Chesapeake Bay, both Envisat acquisition times are close to a local minimum of the wind speed. Therefore, a bias towards underestimating the climatological mean wind speed is expected here. For SAR mean winds at the remaining buoy locations displayed in Figure 6, the effect from diurnal variability will be smaller but still present. Adding more Sentinel-1 acquisitions will even out the diurnal sampling bias from Envisat.

Sea breeze phenomena present in this region are contributing to diurnal wind speed variations (Hughes and Veron, 2015). The influence of the diurnal cycle is more pronounced closer to shore. SAR images that happen to oversample the wind speed minimum of the diurnal cycle would cause a stronger bias towards lower wind speeds closer to shore than farther offshore. Wind observations sampled in such a way would artificially increase the coastal gradient.

e) Wind speed gradients from SAR and ~~the WIND toolkit~~WTK

Mean wind speed maps from ~~the~~SAR and WTK ~~are~~have been compared ~~with seasonally corrected SAR winds~~in this study. Mesoscale models are known to have higher uncertainties offshore if winds come from land (Hahmann et al., 2015). For the buoy locations in Figure 5, westerly winds come across land and the wind roses show that these directions occur frequently. For these directions, coastal wind speed gradients ~~are expected to~~ occur, caused by the roughness change between land and sea. Coastal gradients from SAR have been shown to agree well with lidar wind speeds for the first few kilometers from shore (Ahsbahs et al., 2017). The SAR-based wind atlas has a resolution of 0.02° that makes it ideal for investigating horizontal variations in the mean wind speed and serving as a reference for modelled wind speed gradients from the WTK.

Wind speeds from SAR are typically lower than those from the WTK close to shore but gradients from SAR are higher than from the WTK for most regions (Figure 12b, c, e, and f). At 100 km from ~~shore~~the shoreline, SAR tends to give higher winds than WTK. Wind speed gradients show that SAR winds ~~are~~, on average, ~~showing~~show an increase of 1.40 m/s per 100 km. For the WTK, this value is only 0.91 m/s per 100 km. Fixed times of the satellite tracks could influence wind speed gradients if they show diurnal variability. This cannot easily be investigated from buoy measurements because they lack the spatial coverage, which was the initial motivation for this study. The influence of sampling biases is unlikely the sole source for the observed differences in the wind speed gradients. ~~It seems likely that WTK is underestimating wind speed gradients for the first 100 km but a closer investigation is necessary to confirm this.~~

~~Wind atlases can be used to investigate wind resource potential at large scales; i.e., identifying regions that are most promising for wind farm development. Mean wind speeds at equal distance to shore showed good agreement in the northern part of the domain but disagree more strongly in the south. Results from SAR show much more variation along the coast and a distinct minimum in the wind speed close to Delaware (transect_id from 400 to 500). In this region, results from buoy 44072 located~~

~~at Chesapeake Bay (Figure 7) suggest that Envisat is sampling during two local wind speed minima. This could partially explain the low SAR winds speed in this region. Results from earlier resource assessments in Dvorak et al. (2013) using WRF found that wind resources are generally increasing going further from south to north in our investigated domain but show less variability than both SAR and WTK.~~

A longstanding challenge in SAR wind analysis has been that neutral stratification of the surface layer must be assumed. The effect of this assumed neutral stratification of the surface layer is a wind speed bias that depends on the stability of the atmospheric surface layer. The SAR-derived wind speeds are too low in regions where the surface layer is stable, because wind speed must compensate for the too high (i.e. neutral rather than stable) drag coefficient assumed. Likewise, the SAR-derived wind speeds are too high in regions where the surface layer is unstable, because wind speed must compensate for the too low (i.e. neutral rather than unstable) drag coefficient assumed. Basically, the SAR-derived wind is having to compensate for the lack of the stability dependence of the vertical mixing of momentum in the surface layer. This is reflected in our study in the observation that SAR winds are faster than buoy winds over the Gulf Stream (where the atmospheric surface layer is destabilized by the warm underlying water) and slower than the buoy winds over the cold waters north of the Gulf Stream (where the atmospheric surface layer is stabilized by the cool underlying water). Results from earlier resource assessments in Dvorak et al. (2013) using WRF show that wind resources are generally increasing going from south to north in our investigated domain but show less variability than both SAR and WTK.

Spatial ~~variation~~variations of the mean wind speed within lease areas for wind farm development ~~is~~have been investigated using ~~WTK~~the SAR and ~~SAR~~WTK data (Figure 15). For most areas, WTK shows less variation than SAR. For example, mean wind speeds from the WTK for "New Jersey South" range from 6.8 to 7.0 m/s. Low variation like this might lead a developer to neglect horizontal wind speed gradients at their site; i.e., during the planning of a measurement campaign. At the same location, SAR wind speeds range from 6.3 to 7.1 m/s. This variation is substantially larger, suggesting that wind speed variation within this area should be considered. SAR wind maps resolve more variation than mesoscale models or scatterometers, which can explain part of the increased variation (Karagali et al., 2014). Another reason could be speckle noise in the SAR images themselves but spatial and temporal averaging, as performed in this study, will greatly reduce this effect. Variations found here are in line with previous studies from the Anholt wind farm in Denmark, which is located downstream of a complex coastline and can experience strong wind speed gradients (Ahsbahs et al., 2018; Peña et al., 2017).

f) Future work

~~We see two ways forward for using SAR-derived wind atlases for mesoscale model comparisons: i) improving the climatological representativeness of the SAR wind atlas, and ii) dropping the assumption of random sampling of the SAR data and subsample the mesoscale model data to match the sampling characteristics of SAR.~~

~~i) Seasonal biases and poor representation of diurnal cycles are likely major contributors to uncertainty for the SAR wind atlas. We would like to suggest a way to further improve SAR wind atlases to correctly represent climatological conditions.~~

~~Weighting SAR scenes by month could~~This study has utilized the COARE 3.0 bulk flux algorithm to account for the effects of atmospheric stability on the vertical extrapolation of buoy winds. This same stability correction could be used to convert the SAR-derived surface stress to stability-aware SAR winds given that the air-sea temperature difference for any point in the area of interest can be obtained from the WTK data set. The neutral drag law could be used to convert the neutral-equivalent SAR-derived winds to surface stress and then the equations from the COARE 3.0 bulk flux algorithm could be applied to convert that surface stress back to a stability-aware 10 m wind. This would be a major advance for SAR wind analysis and represents a natural next step for our analysis of wind resources along the US East Coast.

With an increasing archive of Sentinel-1 data, future wind atlases will be based on samples, which are more distributed over the time of day. The rapid growth of our SAR data archives over time will in itself improve the accuracy of wind resource statistics. Further, a weighting of the SAR scenes by month could partly overcome seasonal biases and give better estimations of the Weibull parameters while retaining the observational character of ~~the SAR-based wind atlas. Additionally, acquisition times of Envisat and Sentinel-1 are separated by 5 hours as shown in Figure 7. With an increasing archive of Sentinel-1 data, future wind atlases will be based on data more evenly distributed over the time of day.~~

~~ii) The WTK is based on a mesoscale model and does not experience sampling biases because it provides time series data for each point. Instead of assuming the SAR wind atlas to be climatologically representative, we suggest randomly sampling mesoscale model data to more realistically represent the seasons and times of day present in the SAR archive. Repeating this process would create an ensemble of model-based wind atlases including uncertainties from the SAR sampling. The SAR wind atlas can raise awareness for possible flaws in the model where it falls outside the mesoscale model ensemble envelope. This approach could be combined with the investigation of spatial wind speed variability presented in this study.~~a SAR-based wind atlas.

6 Conclusion

Using a large number of collocated buoy measurements, we have shown that SAR wind fields from different sensors can be intercalibrated. The derived SAR wind atlas is novel in two regards: 1) it ensures consistent calibration towards wind retrievals from different sensors, and 2) it covers the US East Coast where a similar product has not been available before. The presented sensors show seasonal sampling biases that are inconsistent over the study domain but mean wind speeds can be corrected to show a bias of 0.09 m/s and an RMSE of 0.39 m/s compared to long-term buoy observations.

Comparisons of the long-term mean wind speeds at 10 m between SAR and WTK indicate that: 1) the model could under-predict the horizontal wind speed gradient with respect to the distance to shore, and 2) wind speed variations within areas designated for offshore wind farm development are lower in the WTK than with SAR. These findings raise awareness that spatial variations of wind resources might be underestimated from in this mesoscale model. SAR-derived wind atlases can serve as independent data sources most useful in the early planning phase of an offshore wind farm project.

~~**Acknowldgements**~~

Acknowledgements

This work was authored [in part] by the National Renewable Energy Laboratory, operated by Alliance for Sustainable Energy, LLC, for the U.S. Department of Energy (DOE) under Contract No. DE-AC36-08GO28308. Funding provided by the U.S. Department of Energy Office of Energy Efficiency and Renewable Energy Wind Energy Technologies Office. The views expressed in the article do not necessarily represent the views of the DOE or the U.S. Government. The U.S. Government retains and the publisher, by accepting the article for publication, acknowledges that the U.S. Government retains a nonexclusive, paid-up, irrevocable, worldwide license to publish or reproduce the published form of this work, or allow others to do so, for U.S. Government purposes. We thank Evan Rosenlieb, Michael Rossol and Paul Doubrawa from the National Renewable Energy Laboratory (NREL) for their input and assistance. We also acknowledge Jane Lockshin from NREL, who created the offshore transects used to examine coastal gradients in wind speed estimates and George Scott who assisted with handling ocean buoy data download from NOAA.

~~**7 References**~~

~~Ahsbahs, T., Badger, M., Karagali, I. and Larsén, X. G.: Validation of Sentinel-1A SAR Coastal Wind Speeds Against Scanning LiDAR, Remote Sens., 9(6), 552, doi:10.3390/rs9060552, 2017.~~

~~Ahsbahs, T., Badger, M., Volker, P., Hansen, K. S. and Hasager, C. B.: Applications of satellite winds for the offshore wind farm site Anholt, Wind Energy Sci., 3, 573–588, doi:10.5194/wes-3-573-2018, 2018.~~

~~Badger, M., Badger, J., Nielsen, M., Hasager, C. B. and Peña, A.: Wind class sampling of satellite SAR imagery for offshore wind resource mapping, J. Appl. Meteorol. Climatol., 49(12), 2474–2491, doi:10.1175/2010JAMC2523.1, 2010.~~

~~Badger, M., Peña, A., Hahmann, A. N., Mouche, A. A. and Hasager, C. B.: Extrapolating Satellite Winds to Turbine Operating Heights, J. Appl. Meteorol. Climatol., 55(4), 975–991, doi:10.1175/JAMC-D-15-0197.1, 2016.~~

~~Badger, M., Ahsbahs, T., Maule, P. and Karagali, I.: Inter-calibration of SAR data series for offshore wind resource assessment – in preparation, Remote Sens. Environ., 2019.~~

~~Barthelmie, R. J. and Pryor, S. C.: Can Satellite Sampling of Offshore Wind Speeds Realistically Represent Wind Speed Distributions?, J. Appl. Meteorol., 42(1), 83–94, doi:10.1175/1520-0450(2003)042<0083:CSSOOW>2.0.CO;2, 2003.~~

~~Barthelmie, R. J., Badger, J., Pryor, S. C., Hasager, C. B., Christiansen, M. B. and Jørgensen, B. H.: Offshore Coastal Wind Speed Gradients: issues for the design and development of large offshore windfarms, Wind Eng., 31(6), 369–382, doi:10.1260/030952407784079762, 2007.~~

~~BOEM: Outer continental shelf drilling. [online] Available from: http://www.defenders.org, 2018.~~

~~Christiansen, M. B., Koch, W., Horstmann, J., Hasager, C. B. and Nielsen, M.: Wind resource assessment from C-band SAR,~~

~~Remote Sens. Environ., 105(1), 68–81, doi:10.1016/j.rse.2006.06.005, 2006.~~

~~Colle, B. A., Sienkiewicz, M. J., Archer, C., Veron, D., Veron, F., Kempton, W. and Mak, J. E.: Improving the Mapping and Predition of Offshore Wind Resources (IMPOWR), Bull. Am. Meteorol. Soc., (August), 1377–1390, 2016.~~

~~Doubrawa, P., Barthelmie, R. J., Pryor, S. C., Hasager, C. B. and Badger, M.: Satellite winds as a tool for offshore wind resource assessment : The Great Lakes Wind Atlas, Remote Sens. Environ., 168, 349–359, doi:10.1016/j.rse.2015.07.008, 2015.~~

~~Draxl, C., Hodge, B. and Clifton, A.: Overview and Meteorological Validation of the Wind Integration National Dataset Toolkit, Golden., 2015a.~~

~~Draxl, C., Clifton, A., Hodge, B. and Mccaa, J.: The Wind Integration National Dataset (WIND) Toolkit The Wind Integration National Dataset (WIND) Toolkit, Appl. Energy, 151(August), 355–366, doi:10.1016/j.apenergy.2015.03.121, 2015b.~~

~~Dvorak, M. J., Corcoran, B. A., Hoeve, J. E. Ten, McIntyre, N. G. and Jacobsen, M. Z.: US East Coast offshore wind energy resources and their relationship to peak-time electricity demand, Wind Energy, 16(April), 977–997, doi:10.1002/we.1524, 2013.~~

~~Fairall, C. W., Bradley, E. F., Hare, J. E., Grachev, A. A. and Edson, J. B.: Bulk parameterization of air-sea fluxes: Updates and verification for the COARE algorithm, J. Clim., 16(4), 571–591, doi:10.1175/1520-0442(2003)016<0571:BPOASF>2.0.CO;2, 2003.~~

~~Figa-Saldaña, J., Wilson, J. J. W., Attema, E., Gelsthorpe, R., Drinkwater, M. R. and Stoffelen, A.: Technical Note / Note technique The advanced scatterometer (ASCAT) on the meteorological operational (MetOp) platform : A follow on for European wind scatterometers, Can. J. Remote Sens., 28(3), 404–412, 2002.~~

~~Hahmann, A. N., Vincent, C. L., Peña, A., Lange, J. and Hasager, C. B.: Wind climate estimation using WRF model output: Method and model sensitivities over the sea, Int. J. Climatol., 35(12), 3422–3439, doi:10.1002/joc.4217, 2015.~~

~~Hasager, C. B., Badger, M., Peña, A., Larsén, X. G. and Bingöl, F.: SAR-based wind resource statistics in the Baltic Sea, Remote Sens., 3(1), 117–144, doi:10.3390/rs3010117, 2011.~~

~~Hasager, C. B., Mouche, A., Badger, M., Bingöl, F., Karagali, I., Driesenaar, T., Stoffelen, A., Peña, A. and Longépé, N.: Offshore wind climatology based on synergetic use of Envisat ASAR, ASCAT and QuikSCAT, Remote Sens. Environ., 156, 247–263, doi:10.1016/j.rse.2014.09.030, 2015.~~

~~Hersbach, H.: Comparison of C-Band Scatterometer CMOD5.N Equivalent Neutral Winds with ECMWF, J. Atmos. Ocean. Technol., 27(4), 721–736, doi:10.1175/2009JTECHO698.1, 2010.~~

~~Horstmann, J., Koch, W., Lehner, S. and Tonboe, R.: Ocean winds from RADARSAT-1 ScanSAR, Can. J. Remote Sens., 28(3), 524–533, 2002.~~

~~Hughes, C. P. and Veron, D. E.: Characterization of Low-Level Winds of Southern and Coastal Delaware, J. Appl. Meteorol. Climatol., 54(1), 77–93, doi:10.1175/JAMC-D-14-0011.1, 2015.~~

~~Karagali, I., Peña, A., Badger, M. and Hasager, C. B.: Wind characteristics in the North and Baltic Seas from the QuikSCAT~~

~~satellite, Wind Energy, 17(1), 123–140, doi:10.1002/we.1565, 2014.~~

~~Karagali, I., Hahmann, A. N., Badger, M. and Mann, J.: New European wind atlas offshore, J. Phys. Conf. Ser., 1037, 10, doi:10.1088/1742-6596/1037/5/052007, 2018.~~

~~Kempton, W., Archer, C. L., Dhanju, A., Garvine, R. W. and Jacobson, M. Z.: Large CO2 reductions via offshore wind power matched to inherent storage in energy end-uses, Geophys. Res. Lett., 34(2), 1–5, doi:10.1029/2006GL028016, 2007.~~

~~Lu, Y., Zhang, B., Member, S., Perrie, W., Aur, A., Li, X., Member, S. and Wang, H.: A C-Band Geophysical Model Function for Determining Coastal Wind Speed Using Synthetic Aperture Radar, IEEE J. Sel. Top. Appl. Earth Obs. Remote Sens., 11(7), 2417–2428, doi:10.1109/JSTARS.2018.2836661, 2018.~~

~~Miranda, N.: S-1A TOPS Radiometric Calibration Refinement # 1. [online] Available from: https://sentinel.esa.int/documents/247904/2142675/Sentinel-1A_TOPS_Radiometric_Calibration_Refinement, 2015.~~

~~Monaldo, F.: Expected differences between buoy and radar altimeter estimates of wind speed and significant wave height and their implications on buoy-altimeter comparisons, J. Geophys. Res., 93(C3), 2285–2302, doi:10.1029/JC093iC03p02285, 1988.~~

~~Monaldo, F. M.: Maryland Offshore Wind Climatology with Application to Wind Power Generation, Laurel., 2011.~~

~~Monaldo, F. M., Li, X., Pichel, W. G. and Jackson, C. R.: Ocean wind speed climatology from spaceborne SAR imagery, Bull. Am. Meteorol. Soc., 95(4), 565–569, doi:10.1175/BAMS-D-12-00165.1, 2014.~~

~~Mouche, A. A., Hauser, D., Daloze, J. F. and Guérin, C.: Dual-polarization measurements at C-band over the ocean: Results from airborne radar observations and comparison with ENVISAT ASAR data, IEEE Trans. Geosci. Remote Sens., 43(4), 753–769, doi:10.1109/TGRS.2005.843951, 2005.~~

~~National Data Buoy Center: eteorological and oceanographic data collected from the National Data Buoy Center Coastal-Marine Automated Network (C-MAN) and moored (weather) buoys. National Oceanographic Data Center, NOAA. Dataset, 1971.~~

~~National Data Buoy Center: Handbook of Automated Data Quality Control Checks and Procedures, Mississippi. [online] Available from: http://www.ndbc.noaa.gov/NDBCHandbookofAutomatedDataQualityControl2009.pdf, 2009.~~

~~National Data Buoy Center: NDBC Web Data Guide NDBC Web Data Guide, Mississippi. [online] Available from: https://www.ndbc.noaa.gov/docs/ndbc_web_data_guide.pdf, 2015.~~

~~Peña, A., Schaldemose Hansen, K., Ott, S. and Van Der Laan, M. P.: On wake modeling, wind-farm gradients and AEP predictions at the Anholt wind farm, Wind Energy Sci. Discuss., 2017, 1–18, doi:10.5194/wes-2017-37, 2017.~~

~~Pryor, S. C., Nielsen, M., Barthelmie, R. J. and Mann, J.: Can Satellite Sampling of Offshore Wind Speeds Realistically Represent Wind Speed Distributions? Part II: Quantifying Uncertainties Associated with Distribution Fitting Methods, J. Appl. Meteorol., 42(1), 83–94, doi:10.1175/1520-0450(2003)042<0083:CSSOOW>2.0.CO;2, 2003.~~

~~Sandven, S., Johannessen, O. M., Miles, M. W., Pettersson, L. H. and Kloster, K.: Barents Sea seasonal ice zone features and~~

~~processes from ERS 1 synthetic aperture radar: Seasonal Ice Zone Experiment 1992, J. Geophys. Res., 104(C7), 15843–15857, doi:Doi 10.1029/1998jc900050, 1999.~~

~~Stoffelen, A. and Anderson, D.: Scatterometer data interpretation: Estimation and validation of the transfer function CMOD4, J. Geophys. Res., 102(C3), 5767–2780, doi:10.1029/96JC02860, 1997.~~

~~Takeyama, Y., Ohsawa, T., Kozai, K., Hasager, C. B. and Badger, M.: Comparison of geophysical model functions for SAR wind speed retrieval in japanese coastal waters, Remote Sens., 5(4), 1956–1973, doi:10.3390/rs5041956, 2013.~~

~~Troen, I. and Petersen, E. L.: European Wind Atlas, Risø National Laboratory, Roskilde., 1989.~~

~~Troitskaya, Y., Abramov, V., Baidakov, G., Ermakova, O., Zuikova, E., Sergeev, D., Ermoshkin, A., Kazakov, V., Kandaurov, A., Rusakov, N., Poplavsky, E. and Vdovin, M.: Cross-Polarization GMF For High Wind Speed and Surface Stress Retrieval, J. Geophys. Res. Ocean., doi:10.1029/2018JC014090, 2018.~~

~~Vachon, P. W., Wolfe, J. and Hawkins, R. K.: The impact of RADARSAT ScanSAR Image Quality on Ocean Wind Retrieval, in SAR Workshop: CEOS Committee on Earth Observation Satellites; Working Group on Calibration and Validation, vol. 429, pp. 519–524, Wuropean Space Agency, Paris., 1999.~~

~~Valenzuela, G. R.: Theories for the interaction of electromagnetic and oceanic waves–A review, Boundary-Layer Meteorol., 13(1), 61–85, doi:10.1007/BF00913863, 1978.~~

~~Wind Europe: Offshore Wind in Europe: Key trends and statistics. [online] Available from: https://windeurope.org/wp-content/uploads/files/about-wind/statistics/WindEurope-Annual-Offshore-Statistics-2017.pdf, 2018.~~

Data availability

The SAR wind atlas derived in this study is available under https://doi.org/10.11583/DTU.11636511.v1 (Ahsbahs and Badger, 2020).

7 Reference

Ahsbahs, T., Badger, M., Karagali, I. and Larsén, X. G.: Validation of Sentinel-1A SAR Coastal Wind Speeds Against Scanning LiDAR, Remote Sens., 9(6), 552, doi:10.3390/rs9060552, 2017.

Ahsbahs, T., Badger, M., Volker, P., Hansen, K. S. and Hasager, C. B.: Applications of satellite winds for the offshore wind farm site Anholt, Wind Energy Sci., 3, 573–588, doi:10.5194/wes-3-573-2018, 2018.

Ahsbahs, Tobias Torben; Badger, Merete (2020): SAR wind atlas US East Coast. Technical University of Denmark. Dataset. https://doi.org/10.11583/DTU.11636511.v1

Badger, M., Badger, J., Nielsen, M., Hasager, C. B. and Peña, A.: Wind class sampling of satellite SAR imagery for offshore wind resource mapping, J. Appl. Meteorol. Climatol., 49(12), 2474–2491, doi:10.1175/2010JAMC2523.1, 2010.

Badger, M., Peña, A., Hahmann, A. N., Mouche, A. A. and Hasager, C. B.: Extrapolating Satellite Winds to Turbine Operating Heights, J. Appl. Meteorol. Climatol., 55(4), 975–991, doi:10.1175/JAMC-D-15-0197.1, 2016.

Badger, M., Ahsbahs, T. T., Maule, P., & Karagali, I. (2019). Inter-calibration of SAR data series for offshore wind resource assessment. Remote Sensing of Environment, 232, 111316. https://doi.org/10.1016/j.rse.2019.111316.

Barthelmie, R. J. and Pryor, S. C.: Can Satellite Sampling of Offshore Wind Speeds Realistically Represent Wind Speed Distributions?, J. Appl. Meteorol., 42(1), 83–94, doi:10.1175/1520-0450(2003)042<0083:CSSOOW>2.0.CO;2, 2003.

Barthelmie, R. J., Badger, J., Pryor, S. C., Hasager, C. B., Christiansen, M. B. and Jørgensen, B. H.: Offshore Coastal Wind Speed Gradients: issues for the design and development of large offshore windfarms, Wind Eng., 31(6), 369–382, doi:10.1260/030952407784079762, 2007.

BOEM: Outer continental shelf drilling. [online] Available from: http://www.defenders.org, 2018.

Charnock, H. (1955). Wind stress on a water surface. *Quart. J. Roy. Meteor. Soc.*, **81**, 639–640.

Christiansen, M. B., Koch, W., Horstmann, J., Hasager, C. B. and Nielsen, M.: Wind resource assessment from C-band SAR, Remote Sens. Environ., 105(1), 68–81, doi:10.1016/j.rse.2006.06.005, 2006.

Colle, B. A., Sienkiewicz, M. J., Archer, C., Veron, D., Veron, F., Kempton, W. and Mak, J. E.: Improving the Mapping and Predition of Offshore Wind Resources (IMPOWR), Bull. Am. Meteorol. Soc., (August), 1377–1390, 2016.

Doubrawa, P., Barthelmie, R. J., Pryor, S. C., Hasager, C. B. and Badger, M.: Satellite winds as a tool for offshore wind resource assessment : The Great Lakes Wind Atlas, Remote Sens. Environ., 168, 349–359, doi:10.1016/j.rse.2015.07.008, 2015.

Draxl, C., Hodge, B. and Clifton, A.: Overview and Meteorological Validation of the Wind Integration National Dataset Toolkit, Golden., 2015a.

Draxl, C., Clifton, A., Hodge, B. and Mccaa, J.: The Wind Integration National Dataset (WIND) Toolkit The Wind Integration National Dataset (WIND) Toolkit, Appl. Energy, 151(August), 355–366, doi:10.1016/j.apenergy.2015.03.121, 2015b.

Dvorak, M. J., Corcoran, B. A., Hoeve, J. E. Ten, McIntyre, N. G. and Jacobsen, M. Z.: US East Coast offshore wind energy resources and their relationship to peak-time electricity demand, Wind Energy, 16(April), 977–997, doi:10.1002/we.1524, 2013.

Fairall, C. W., Bradley, E. F., Hare, J. E., Grachev, A. A. and Edson, J. B.: Bulk parameterization of air-sea fluxes: Updates and verification for the COARE algorithm, J. Clim., 16(4), 571–591, doi:10.1175/1520-0442(2003)016<0571:BPOASF>2.0.CO;2, 2003.

Figa-Saldaña, J., Wilson, J. J. W., Attema, E., Gelsthorpe, R., Drinkwater, M. R. and Stoffelen, A.: Technical Note / Note technique The advanced scatterometer (ASCAT) on the meteorological operational (MetOp) platform : A follow on for European wind scatterometers, Can. J. Remote Sens., 28(3), 404–412, 2002.

Hahmann, A. N., Vincent, C. L., Peña, A., Lange, J. and Hasager, C. B.: Wind climate estimation using WRF model output: Method and model sensitivities over the sea, Int. J. Climatol., 35(12), 3422–3439, doi:10.1002/joc.4217, 2015.

Hasager, C. B., Badger, M., Peña, A., Larsén, X. G. and Bingöl, F.: SAR-based wind resource statistics in the Baltic Sea, Remote Sens., 3(1), 117–144, doi:10.3390/rs3010117, 2011.

Hasager, C. B., Mouche, A., Badger, M., Bingöl, F., Karagali, I., Driesenaar, T., Stoffelen, A., Peña, A. and Longépé, N.: Offshore wind climatology based on synergetic use of Envisat ASAR, ASCAT and QuikSCAT, Remote Sens. Environ., 156, 247–263, doi:10.1016/j.rse.2014.09.030, 2015.

Hersbach, H.: Comparison of C-Band Scatterometer CMOD5.N Equivalent Neutral Winds with ECMWF, J. Atmos. Ocean. Technol., 27(4), 721–736, doi:10.1175/2009JTECHO698.1, 2010.

Horstmann, J., Koch, W., Lehner, S. and Tonboe, R.: Ocean winds from RADARSAT-1 ScanSAR, Can. J. Remote Sens., 28(3), 524–533, 2002.

Hughes, C. P. and Veron, D. E.: Characterization of Low-Level Winds of Southern and Coastal Delaware, J. Appl. Meteorol. Climatol., 54(1), 77–93, doi:10.1175/JAMC-D-14-0011.1, 2015.

Karagali, I., Peña, A., Badger, M. and Hasager, C. B.: Wind characteristics in the North and Baltic Seas from the QuikSCAT satellite, Wind Energy, 17(1), 123–140, doi:10.1002/we.1565, 2014.

Karagali, I., Hahmann, A. N., Badger, M. and Mann, J.: New European wind atlas offshore, J. Phys. Conf. Ser., 1037, 10, doi:10.1088/1742-6596/1037/5/052007, 2018.

Kempton, W., Archer, C. L., Dhanju, A., Garvine, R. W. and Jacobson, M. Z.: Large CO2 reductions via offshore wind power matched to inherent storage in energy end-uses, Geophys. Res. Lett., 34(2), 1–5, doi:10.1029/2006GL028016, 2007.

Lu, Y., Zhang, B., Member, S., Perrie, W., Aur, A., Li, X., Member, S. and Wang, H.: A C-Band Geophysical Model Function for Determining Coastal Wind Speed Using Synthetic Aperture Radar, IEEE J. Sel. Top. Appl. Earth Obs. Remote Sens., 11(7), 2417–2428, doi:10.1109/JSTARS.2018.2836661, 2018.

Miranda, N.: S-1A TOPS Radiometric Calibration Refinement # 1. [online] Available from: https://sentinel.esa.int/documents/247904/2142675/Sentinel-1A_TOPS_Radiometric_Calibration_Refinement, 2015.

Monaldo, F.: Expected differences between buoy and radar altimeter estimates of wind speed and significant wave height and their implications on buoy-altimeter comparisons, J. Geophys. Res., 93(C3), 2285–2302, doi:10.1029/JC093iC03p02285, 1988.

Monaldo, F. M.: Maryland Offshore Wind Climatology with Application to Wind Power Generation, Laurel., 2011.

Monaldo, F. M., Li, X., Pichel, W. G. and Jackson, C. R.: Ocean wind speed climatology from spaceborne SAR imagery, Bull. Am. Meteorol. Soc., 95(4), 565–569, doi:10.1175/BAMS-D-12-00165.1, 2014.

Mouche, A. A., Hauser, D., Daloze, J. F. and Guérin, C.: Dual-polarization measurements at C-band over the ocean: Results from airborne radar observations and comparison with ENVISAT ASAR data, IEEE Trans. Geosci. Remote Sens., 43(4), 753–

769, doi:10.1109/TGRS.2005.843951, 2005.
National Data Buoy Center: eteorological and oceanographic data collected from the National Data Buoy Center Coastal-Marine Automated Network (C-MAN) and moored (weather) buoys. National Oceanographic Data Center, NOAA. Dataset, 1971.
National Data Buoy Center: Handbook of Automated Data Quality Control Checks and Procedures, Mississippi. [online] Available from: http://www.ndbc.noaa.gov/NDBCHandbookofAutomatedDataQualityControl2009.pdf, 2009.
National Data Buoy Center: NDBC Web Data Guide NDBC Web Data Guide, Mississippi. [online] Available from: https://www.ndbc.noaa.gov/docs/ndbc_web_data_guide.pdf, 2015.
Peña, A., Schaldemose Hansen, K., Ott, S. and Van Der Laan, M. P.: On wake modeling, wind-farm gradients and AEP predictions at the Anholt wind farm, Wind Energy Sci. Discuss., 2017, 1–18, doi:10.5194/wes-2017-37, 2017.
Pryor, S. C., Nielsen, M., Barthelmie, R. J. and Mann, J.: Can Satellite Sampling of Offshore Wind Speeds Realistically Represent Wind Speed Distributions? Part II: Quantifying Uncertainties Associated with Distribution Fitting Methods, J. Appl. Meteorol., 42(1), 83–94, doi:10.1175/1520-0450(2003)042<0083:CSSOOW>2.0.CO;2, 2003.
Sandven, S., Johannessen, O. M., Miles, M. W., Pettersson, L. H. and Kloster, K.: Barents Sea seasonal ice zone features and processes from ERS 1 synthetic aperture radar: Seasonal Ice Zone Experiment 1992, J. Geophys. Res., 104(C7), 15843–15857, doi:Doi 10.1029/1998jc900050, 1999.
Stoffelen, A. and Anderson, D.: Scatterometer data interpretation: Estimation and validation of the transfer function CMOD4, J. Geophys. Res., 102(C3), 5767–2780, doi:10.1029/96JC02860, 1997.
Takeyama, Y., Ohsawa, T., Kozai, K., Hasager, C. B. and Badger, M.: Comparison of geophysical model functions for SAR wind speed retrieval in japanese coastal waters, Remote Sens., 5(4), 1956–1973, doi:10.3390/rs5041956, 2013.
Troen, I. and Petersen, E. L.: European Wind Atlas, Risø National Laboratory, Roskilde., 1989.
Troitskaya, Y., Abramov, V., Baidakov, G., Ermakova, O., Zuikova, E., Sergeev, D., Ermoshkin, A., Kazakov, V., Kandaurov, A., Rusakov, N., Poplavsky, E. and Vdovin, M.: Cross-Polarization GMF For High Wind Speed and Surface Stress Retrieval, J. Geophys. Res. Ocean., doi:10.1029/2018JC014090, 2018.
Vachon, P. W., Wolfe, J. and Hawkins, R. K.: The impact of RADARSAT ScanSAR Image Quality on Ocean Wind Retrieval, in SAR Workshop: CEOS Committee on Earth Observation Satellites; Working Group on Calibration and Validation, vol. 429, pp. 519–524, Wuropean Space Agency, Paris., 1999.
Valenzuela, G. R.: Theories for the interaction of electromagnetic and oceanic waves−A review, Boundary-Layer Meteorol., 13(1), 61–85, doi:10.1007/BF00913863, 1978.
Wind Europe: Offshore Wind in Europe: Key trends and statistics. [online] Available from: https://windeurope.org/wp-content/uploads/files/about-wind/statistics/WindEurope-Annual-Offshore-Statistics-2017.pdf, 2018.